Neutron Stars and NuSTAR

A Systematic Survey of Neutron Star Masses in High Mass X-ray Binaries

&

Characterization of CdZnTe Detectors for NuSTAR

A Thesis by
Varun B. Bhalerao
Advisors
Professors Fiona Harrison & Shri R. Kulkarni

In Partial Fulfillment of the Requirements
for the Degree of
Doctor of Philosophy

California Institute of Technology
Pasadena, California

2012

(Defended May 24, 2012)

Dedicated to my parents,
Erawati and Bhalchandra Bhalerao
my role models, motivation,
and strength.

Acknowledgments

My six years at Caltech have been an amazing experience, in both work and personal life. As I write this thesis summarizing the work, it is fitting that I begin by thanking the many people who have made my little achievement possible.

I am very fortunate to have Professors Fiona Harrison and Shri Kulkarni as my advisors. Their foresight, work ethic, and complementary styles of mentoring provided all the ingredients necessary to take me through my thesis. They have provided all resources I needed, and key insights whenever I was short on ideas (or had too many). I have learned a lot from working with them, and will continue striving to live up to their standards.

Working on NuSTAR has been a dream come true. No, really. Who has not wanted to build and launch a satellite? My work would have been impossible without significant help from my lab partners Brian Grefenstette and Vikram Rana. As the junior-most member in the Caltech NuSTAR team, I was the least experienced. I am grateful to Eric Bellm, Jill Burnham, Rick Cook, Takao Kitaguchi, Kristin Madsen, Peter Mao, and Hiromasa Miyasaka for helping me whenever I was stuck. I thank Peter's dentist. Miles Robinson, Steve Stryker, and Robert Crabill have been wonderful troubleshooters and the go-to people for any work in the laboratory. Summer projects by students Nancy Wu and Suk Sien Tie laid good foundations for my future work.

As an electrical engineer, I had a lot to learn about astronomy. My foray into observations was possible thanks to the enthusiastic guidance of Mansi Kasliwal. I thank Professor Marten van Kerkwijk for teaching me how to extract every last bit of information from data—a skill I still strive to perfect. Brad Cenko was extremely helpful in my first year photometer project. I thank Mike Muno for his early work on radial velocities of high mass X-ray binaries, which developed into my observational project. My batchmates Laura, Walter, Matthew, and Yacine have been a constant source of support and inspiration at

Caltech. My work would have been nowhere as much fun without my long-time officemates Gwen and Laura. Together with Mansi, Shriharsh, Swarnima, and Abhilash, they made work a lot of fun! Shriharsh was the sounding board for new ideas at work. I am glad to have the company of Swarnima, Ryan and Krzysztof to share my passion of outreach and amateur astronomy.

Part of what makes Caltech special is the excellent administrative and technical staff, whose success lies in the fact that they are always in the background. My first-year project and subsequent observing runs and Palomar were a pleasure thanks to Kevin Rykoski, Dipali, and Jean Mueller. I thank Richard Dekany, Dan McKenna, and Jeff Zolkower for support on my first year project. The ADPF group, especially Partrick Shopbell and Anu Mahabal, have maintained an excellent computing infrastructure—giving me freedom from install logs and core dumps. Librarians Lindsay Cleary and Joy Painter always went out of their way to help with procuring and issuing books. Special thanks to the several administrative assistants at Caltech: Debby Miles, Nina Borg, and Caprece Anderson at the Space Radiation Laboratory, Bronagh Glaser at Geology and Planetary Sciences, Gina Armas and Gita Patel in Robinson and Cahill, and Teresita Legaspi at the Registrar's Office. Their untiring efforts ensured that I could focus on my work without ever being bogged down by paperwork.

The reason I can put my work at the forefront is an extremely supportive family. None of this would have been possible without the effort and encouragement of my parents, who have placed me and my career ahead of everything else. Sneha has been my motivation through this final phase of my Ph.D.. My extended family, Shri and Shaila Mate, Prasanna, Madhuri, and Amruta Mate have always been around for me. Games with the badminton group at Caltech were a constant source of refreshment (and exercise!). And finally, my family away from home: Mansi, Prabha, Pinkesh, Jayakrishnan, Sushree, Shriharsh, and Ishwari, who have done everything possible to keep me happy. Thank you. *You're awesome*!

Abstract

My thesis centers around the study of neutron stars, especially those in massive binary systems. To this end, it has two distinct components: the observational study of neutron stars in massive binaries with a goal of measuring neutron star masses and participation in NuSTAR, the first imaging hard X-ray mission, one that is extremely well suited to the study of massive binaries and compact objects in our Galaxy.

The Nuclear Spectroscopic Telescope Array (NuSTAR) is a NASA Small Explorer mission that will carry the first focusing high energy X-ray telescope to orbit. NuSTAR has an order-of-magnitude better angular resolution and has two orders of magnitude higher sensitivity than any currently orbiting hard X-ray telescope. I worked to develop, calibrate, and test `CdZnTe` detectors for NuSTAR. I describe the `CdZnTe` detectors in comprehensive detail here—from readout procedures to data analysis. Detailed calibration of detectors is necessary for analyzing astrophysical source data obtained by the NuSTAR. I discuss the design and implementation of an automated setup for calibrating flight detectors, followed by calibration procedures and results.

Neutron stars are an excellent probe of fundamental physics. The maximum mass of a neutron star can put stringent constraints on the equation of state of matter at extreme pressures and densities. From an astrophysical perspective, there are several open questions in our understanding of neutron stars. What are the birth masses of neutron stars? How do they change in binary evolution? Are there multiple mechanisms for the formation of neutron stars? Measuring masses of neutron stars helps answer these questions. Neutron stars in high-mass X-ray binaries have masses close to their birth mass, providing an opportunity to disentangle the role of "nature" and "nurture" in the observed mass distributions. In 2006, masses had been measured for only six such objects, but this small sample showed the greatest diversity in masses among all classes of neutron star binaries. Intrigued by

this diversity—which points to diverse birth masses—we undertook a systematic survey to measure the masses of neutron stars in nine high-mass X-ray binaries. In this thesis, I present results from this ongoing project.

While neutron stars formed the primary focus of my work, I also explored other topics in compact objects. appendix A describes the discovery and complete characterization of a 1RXS J173006.4+033813, a polar cataclysmic variable. appendix B describes the discovery of a diamond planet orbiting a millisecond pulsar, and our search for its optical counterpart.

Contents

List of Figures

List of Tables

List of Acronyms

ADC: analog-to-digital convertor

AGN: active galactic nuclei

ASIC: application-specific integrated circuit

BH: black hole

cps: counts per second

DBSP: double beam spectrograph

EOS: equation of state

ESD: electrostatic discharge

FITS: flexible image transport system

FOV: field of view

FPGA: field programmable gate array

FPM: focal plane module

FWHM: Full Width at Half Maximum

GUI: graphical user interface

HEASARC: high energy astrophysics science archive research center

HMXB: high-mass X-ray binary

HPD: half power diameter

HV: high voltage

IC: integrated circuit

IR: infrared

LRIS: low resolution imaging spectrograph

MISC: minimum instruction set computer

MOC: mission operations center

NRL: naval research laboratory

NS: neutron star

NuSTAR nuclear spectroscopic telescope array

NuSTARDAS: NuSTAR data analysis software

OGIP: office of guest investigator programs

PH: pulse height

PI: pulse invariant

PMT: photomultiplier tube

PSF: point-spread function

RMF: redistribution matrix file

QE: quantum efficiency

RV: radial velocity

SAA: south atlantic anamoly

SFXT: supergiant fast X-ray transient

SMBH: super massive black hole

SMEX: small explorer

SNR: signal-to-noise ratio

SOC: science operations center

SRL: space radiation laboratory

ToO: target of opportunity

XRB: X-ray binary

Part One: NuSTAR

Characterization of CdZnTe Detectors for NuSTAR

Image: NuSTAR satellite at Orbital Sciences Corporation

NuSTAR

Part Two: Masses of Neutron Stars

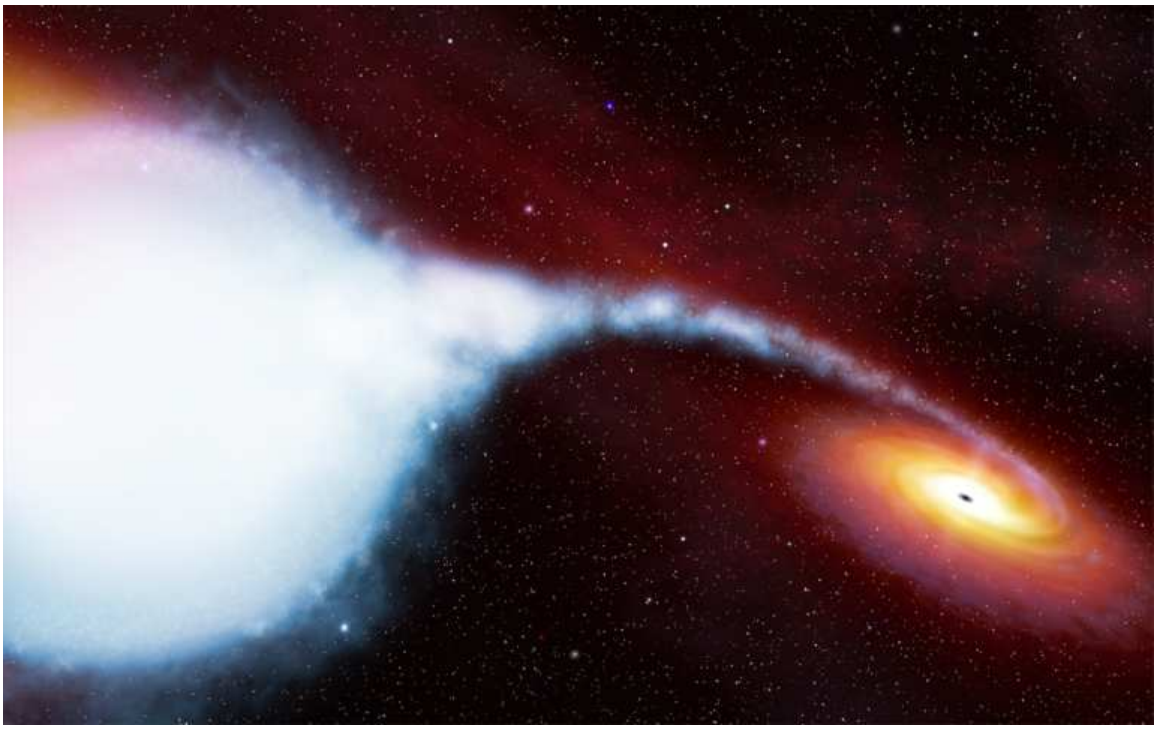

X-Mas: A Search for eXtra Massive Neutron Stars

Image: Artists illustration of a galactic Black Hole High-Mass X-ray Binary Cygnus X-1.

Credit: ESA/Hubble, via Wikimedia Commons.

Neutron Stars

Appendix A

The Polar Catalysmic Variable 1RXS J173006.4+033813

Varun B. Bhalerao[a], Marten H. van Kerkwijk[a,b], Fiona A. Harrison[c], Mansi M. Kasliwal[a], S. R. Kulkarni[a],Vikram R. Rana[c]

[a]Department of Astronomy, California Institute of Technology, Pasadena, CA 91125, USA

[b]On sabbatical leave from Department of Astronomy and Astrophysics, University of Toronto, 50St. George Street, Toronto, ON M5S 3H4, Canada.

[c]Space Radiation Laboratory, California Institute of Technology, Pasadena, CA 91125, USA

Abstract

We report the discovery of 1RXS J173006.4+033813, a polar cataclysmic variable with a period of 120.21 min. The white dwarf primary has a magnetic field of $B = 42\_$ MG, and the secondary is a M3 dwarf. The system shows highly symmetric double peaked photometric modulation in the active state as well as in quiescence. These arise from a combination of cyclotron beaming and ellipsoidal modulation. The projected orbital velocity of the secondary is $K = 390 \pm 4$ km s^{-} . We place an upper limit of 830 ± 65 pc on the distance.

Keywords: binaries: close—binaries: spectroscopic—novae, cataclysmic variables—stars: individiual (1RXS J173006.4+033813)—stars: variables: other

A version of this chapter was published in the *Astrophysical Journal* (Bhalerao et al., 2010). It is reproduced here with permission from AAS.

A.1 Introduction

Cataclysmic Variables (CVs) are close interacting binary systems in which a white dwarf (WD) accretes material from a Roche lobe filling late-type secondary star (Warner, 1995; Hellier, 2001). In most non-magnetic CVs ($B < 10$ G), the material lost from the secondary does not directly fall onto the WD because of its large specific orbital momentum: instead, it settles down in an accretion disc around the WD.

The accretion disc is the brightest component of the CV due to the large gravitational energy release in viscous accretion. The disc dominates the emission from the WD and donor over a wide wavelength range.

On the other hand, the accretion geometry in magnetic CVs is strongly influenced by the WD magnetic field. Magnetic CVs are broadly divided into two subclasses: Polars and Intermediate Polars (IPs). Polars usually show a synchronous or near synchronous rotation of WD with the orbital motion of the binary system and have high magnetic fields ($B > 10$ MG) (for a review, see Cropper, 1990). In IPs the WD rotation is far from synchronous and typically have magnetic field, $B < 10$ MG (for a review, see Hellier, 2002). The strong magnetic field in polars deflects the accretion material from a ballistic trajectory before an accretion disc can form, channeling it to the WD magnetic pole(s). The infalling material forms a shock near the WD surface, which produces radiation from X-rays to infrared wavelengths. Electrons in the ionized shocked region spiral around the magnetic field lines and emit strongly polarized cyclotron radiation at optical and infrared wavelengths. Polars exhibit X-ray on (high) and off (low) states more frequently than the other variety of CVs (Ramsay et al., 2004).

1RXS J173006.4+033813 (hereafter 1RXS J1730+03) is a Galactic source that is highly variable in the optical and X-ray, exhibiting dramatic outbursts of more than 3 magnitudes in optical. It was discovered by the ROSAT satellite during its all-sky survey (Voges et al., 1999). Denisenko et al. (2009), in the course of their investigation of poorly studied ROSAT sources, reported that USNO-B1.0 object 0936-00303814 which is within the $10''$ (radius) localization of the X-ray source showed great variability (ΔR of up to 3 mag) in archival data (Palomar Sky Survey; SkyMorph/NEAT). During certain epochs the source appears to have been undetectable ($m_R > 20$ mag). Denisenko et al. (2009) undertook observations with Kazan State University's 30-cm robotic telescope and found variability on rapid timescales

of 10 minutes.

In this paper, we report the results of our photometric, spectroscopic and X-ray follow-up of 1RXS J1730+03.

A.2 Observations

A.2.1 Optical Photometry

We observed 1RXS J1730+03 with the Palomar Robotic 60-inch telescope (P60; Cenko et al., 2006) from UT 2009 April 17 to UT 2009 June 5, and with the Large Format Camera (LFC; Simcoe et al., 2000) at the 5 m Hale telescope at Palomar on UT 2009 August 26. Here we give details of the photometry.

We define a photometric epoch as observations from a single night when the source could be observed. We obtained 28 epochs with the P60, subject to scheduling and weather constraints. A typical epoch consists of consecutive 90–120 s exposures spanning between 30–300 minutes (Table A.1). We obtained g', r', i' photometry on the first and third epochs. After the third epoch, we continued monitoring the source only in i' band.

We reduced the raw images using the default P60 image analysis pipeline. LFC images were reduced in `IRAF` [1]. We performed photometry using the `IDL DAOPHOT` package (Landsman, 1993). Fluxes of the target and reference stars (Figure A.1) were extracted using the `APER` routine. For aperture photometry, the extraction region was set to one seeing radius, as recommended by Mighell (1999). The sky background was extracted from an annular region 5–15 seeing radii wide. We used flux zero points and seeing values output by the P60 analysis pipeline. Magnitudes for the reference stars were calculated from a few images. The magnitude of 1RXS J1730+03 was calculated relative to the mean magnitude of a 9 reference stars for LFC images, and 15 reference stars for P60 images (Table A.2). The LFC images (Figure A.1) resolve out a faint nearby star ($m_{i'} = 20.8$), $3''.4$ from the target. The median seeing in P60 data is $2''.1$ (Gaussian FWHM): so there is a slight contribution from the flux of this star to photometry of 1RXS J1730+03. We do not correct for this contamination. The statistical uncertainty in magnitudes is $\sim$ 0.2 mag for P60 and

[1] http://iraf.noao.edu/

[2] http://www.ittvis.com/ProductServices/IDL.aspx

Table A.1. Photometry of 1RXS J1730+03

Date (UT)	HJD	Filter name	Exposure time (sec)	Magnitude	Error
20090417	54938.832278	g'	120	20.8	0.13
20090417	54938.835488	i'	90	19.39	0.05
20090417	54938.838696	g'	90	20.75	0.13
20090417	54938.839953	i'	90	19.17	0.05
20090417	54938.841212	g'	90	20.67	0.13
20090417	54938.842469	i'	90	19.1	0.05
20090417	54938.843727	g'	90	20.63	0.12
...	...	...	...	...	...
20090826	55069.691401	$lfci'$	60	20.4	0.05
20090826	55069.693218	$lfci'$	60	20.04	0.06

Note. — This table is available in a machine readable form online. A part of the table is reproduced here for demonstrating the form and content of the table.

Filters g', r' and i' denote data acquired at P60 in the respective filters, $lfci'$ denotes data acquired in the i' band with the Large Format Camera at the Palomar 200" Hale telescope

Relative photometry error. Values do not include an absolute photometry uncertainty of 0.16 mag in the g' band, 0.14 mag in the r' band and 0.06 mag in the i' band. Absolute photometry is derived from default P60 zero point calibrations.

Table A.2. Photometry of reference stars for 1RXS J1730+03

Identifier[a]	Right Ascension	Declination	g' magnitude	r' magnitude	i' magnitude
A	262:30:21.99	03:38:37.5	15.861 ± 0.003	15.600 ± 0.003	15.341 ± 0.003
B	262:30:14.57	03:37:11.0	17.372 ± 0.009	17.153 ± 0.006	16.872 ± 0.008
C, 10	262:32:45.57	03:37:17.0	16.879 ± 0.006	16.691 ± 0.005	16.423 ± 0.006
D, 9	262:32:13.84	03:38:03.0	18.161 ± 0.016	17.929 ± 0.010	17.660 ± 0.013
E	262:31:00.31	03:38:31.3	18.518 ± 0.020	17.462 ± 0.007	16.811 ± 0.007
F	262:30:55.06	03:37:26.4	18.530 ± 0.022	18.158 ± 0.012	17.816 ± 0.016
G, 8	262:31:57.98	03:38:03.9	18.621 ± 0.022	18.259 ± 0.012	17.905 ± 0.016
H	262:30:41.22	03:38:32.8	16.770 ± 0.006	16.081 ± 0.004	15.688 ± 0.004
I	262:29:45.31	03:38:43.7	17.661 ± 0.011	17.302 ± 0.007	16.969 ± 0.008
1	262:32:01.97	03:40:28.3	···	···	17.059 ± 0.035
2	262:31:44.94	03:39:48.6	···	···	19.855 ± 0.043
3	262:32:31.60	03:39:32.4	···	···	19.148 ± 0.039
4	262:32:33.94	03:38:59.4	···	···	17.622 ± 0.033
5	262:32:11.15	03:38:39.0	···	···	20.777 ± 0.049
6	262:31:35.94	03:38:29.5	···	···	19.843 ± 0.026
7	262:31:07.21	03:37:57.9	···	···	19.057 ± 0.026
11	262:31:55.09	03:36:45.4	···	···	17.471 ± 0.030
12	262:31:40.33	03:36:34.5	···	···	16.339 ± 0.044
13	262:33:19.44	03:36:21.2	···	···	18.006 ± 0.030
14	262:31:45.44	03:36:12.4	···	···	18.085 ± 0.048
15	262:32:18.64	03:35:48.1	···	···	17.392 ± 0.055

[a]

[b] g'

r' i'

$\sim$ 0.05 mag for LFC, and the systematic uncertainty is 0.16 mag in the g' band, 0.14 mag in the r' band and 0.06 mag in the i' band.

The resultant lightcurves are shown in Figures A.2, A.3 & A.4. Table A.1 provides the photometry.

A.2.2 Spectroscopy

We obtained optical and near-infrared spectra of 1RXS J1730+03 at various stages after outburst (Figure A.5). The first optical spectra were taken 13 days after the first photometric epoch. We used the Low Resolution Imaging Spectrograph on the 10 m Keck-I telescope (LRIS; Oke et al., 1995), with upgraded blue camera (McCarthy et al., 1998; Steidel et al., 2004), covering a wavelength range from 3,200 Å – 9,200 Å. We acquired more optical data 34 days after outburst, with the Double Beam Spectrograph on the 5 m Hale telescope at Palomar (DBSP; Oke & Gunn, 1982). We took 5 exposures spanning one complete photometric period, covering the 3,500 Å – 10,000 Å wavelength range. We took late time spectra covering just over one photometric period for the quiescent source with the upgraded LRIS . At this epoch, we aligned the slit at a position angle of 45 degrees to cover both the target and the contaminator, 3″.4 to its South West (Figure A.1). We also obtained low resolution J-band spectra with the Near InfraRed Spectrograph on the 10 m Keck-II telescope (NIRSPEC; McLean et al., 1998). 12 spectra of 5 minutes each were acquired, covering the wavelength region from 11,500 Å – 13,700 Å. For details of the observing set up, see the notes to Table A.5.

We analyzed the spectra using `IRAF` and `MIDAS` and flux calibrated them using appropriate standards. Wavelength solutions were obtained using arc lamps and with offsets determined from sky emission lines. Figure A.6 shows an optical spectrum from each epoch, while the IR spectrum is shown in Figure A.7.

The second LRIS epoch had variable sky conditions. Here, we extracted spectra of the aforementioned contaminator. This object is also a M-dwarf, hence both target and contaminator spectra will be similarly affected by the atmosphere. We estimate the i' magnitude of the contaminator in each spectrum, and compare it to the the value measured

[3] http://www2.keck.hawaii.edu/inst/lris/lris-red-upgrade-notes.html

[4] Munich Image Data Analysis System; http://www.eso.org/sci/data-processing/software/esomidas/

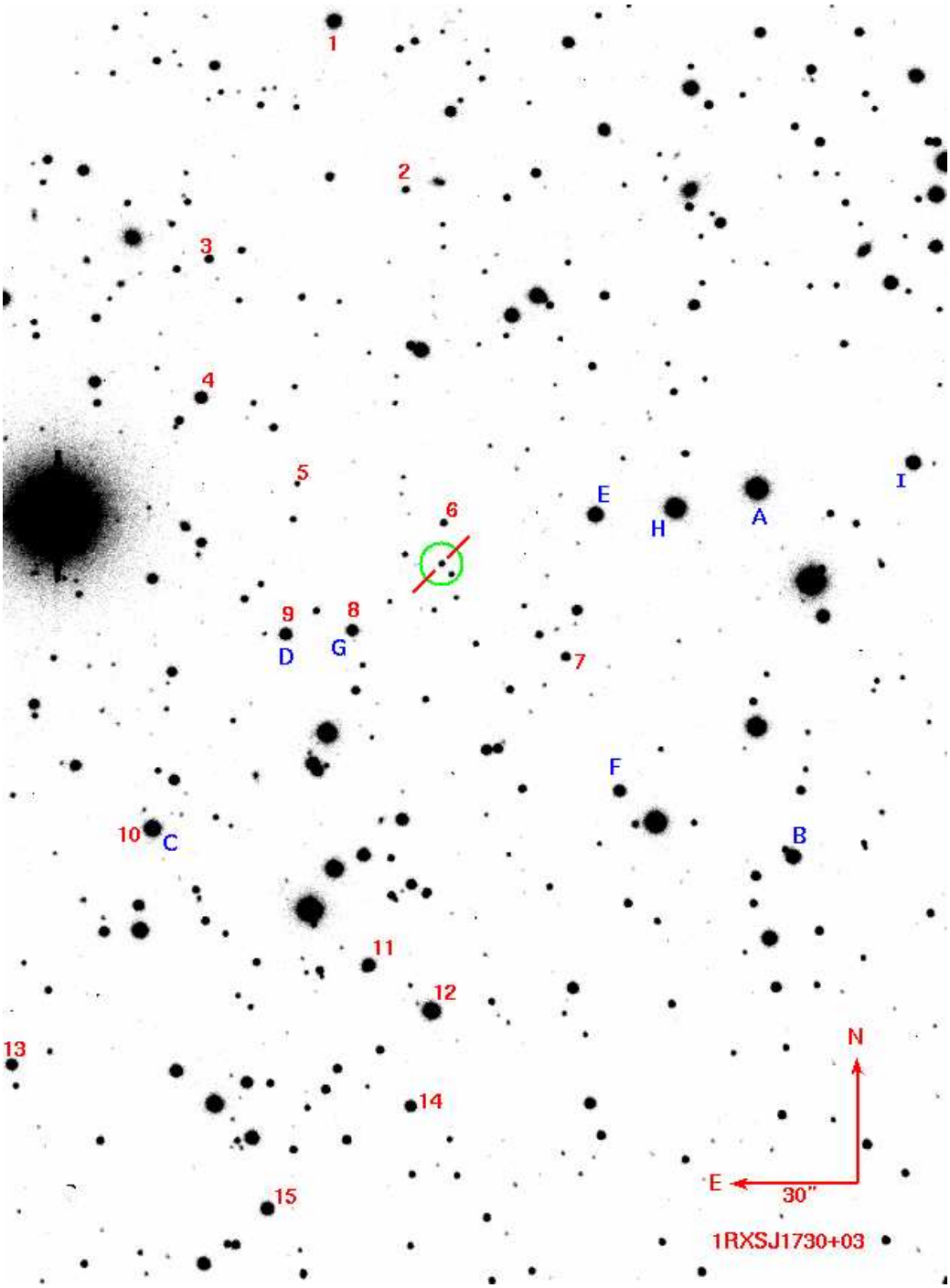

Figure A.1. Finder chart for 1RXS J1730+03 ($\alpha = 17^{\rm h}30^{\rm m}06^{\rm s}.19$, $\delta = +03°38'18''.8$). This i' band image was acquired with the Large Format Camera (LFC) at the 5 m Hale telescope at Palomar. Stars numbered 1–15 in red are used for relative photometry in LFC data. Stars labeled `A`–`I` in blue are used for relative photometry in P60 data (Section A.2.1). The green circle shows the $5''$ extraction region used for calculating UVOT fluxes. The circle includes a contaminator, $3''.4$ to the South-West of the target.

Table A.3. Observation log for *Swift* ToO observations of 1RXS J1730+03.

Obs ID	Start Date & Time	Stop Time	Exposure (s)	Filter	Wavelength (Å)	Magnitude	Flux	Flux (μJy)
00035571001	2006 Feb 9 16:56:43	18:42:00	1106	UVM2	2231	17.9±0.1	31±2	51±3
				XRT			0.02	0.06 (5 keV)
00031408001	2009 May 3 18:28:56	19:02:12	1964	UVM2	2231	20.44±0.21	3.04±0.59	5.05±0.99
00031408002	2009 May 4 18:34:04	22:12:54	4896	UVW1	2634	20.14±0.10	3.47±0.32	8.04±0.75
00031408003	2009 May 6 03:02:21	15:36:33	5621	UVW2	2030	21.48±0.17	1.38±0.22	1.93±0.30
				XRT			<0.002	<0.006 (5 keV)

Effective wavelength for each filter for a Vega-like spectrum (Poole et al., 2007).

Flux in the units of 10^{-} erg cm^{-} s^{-} A^{-} .

Counts s^{-} in 0.5-10 keV.

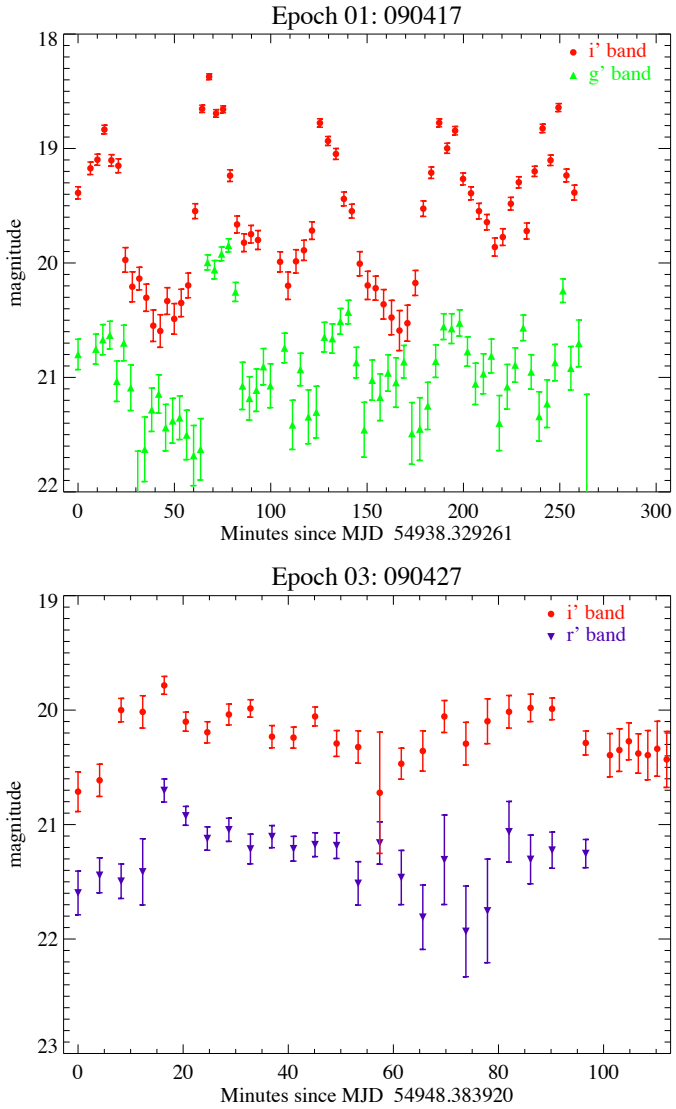

Figure A.2. P60 photometry of 1RXS J1730+03. Top panel: Epoch 1 photometry in g' and i' bands. Bottom panel: Epoch 3 photometry in r' and i' bands.

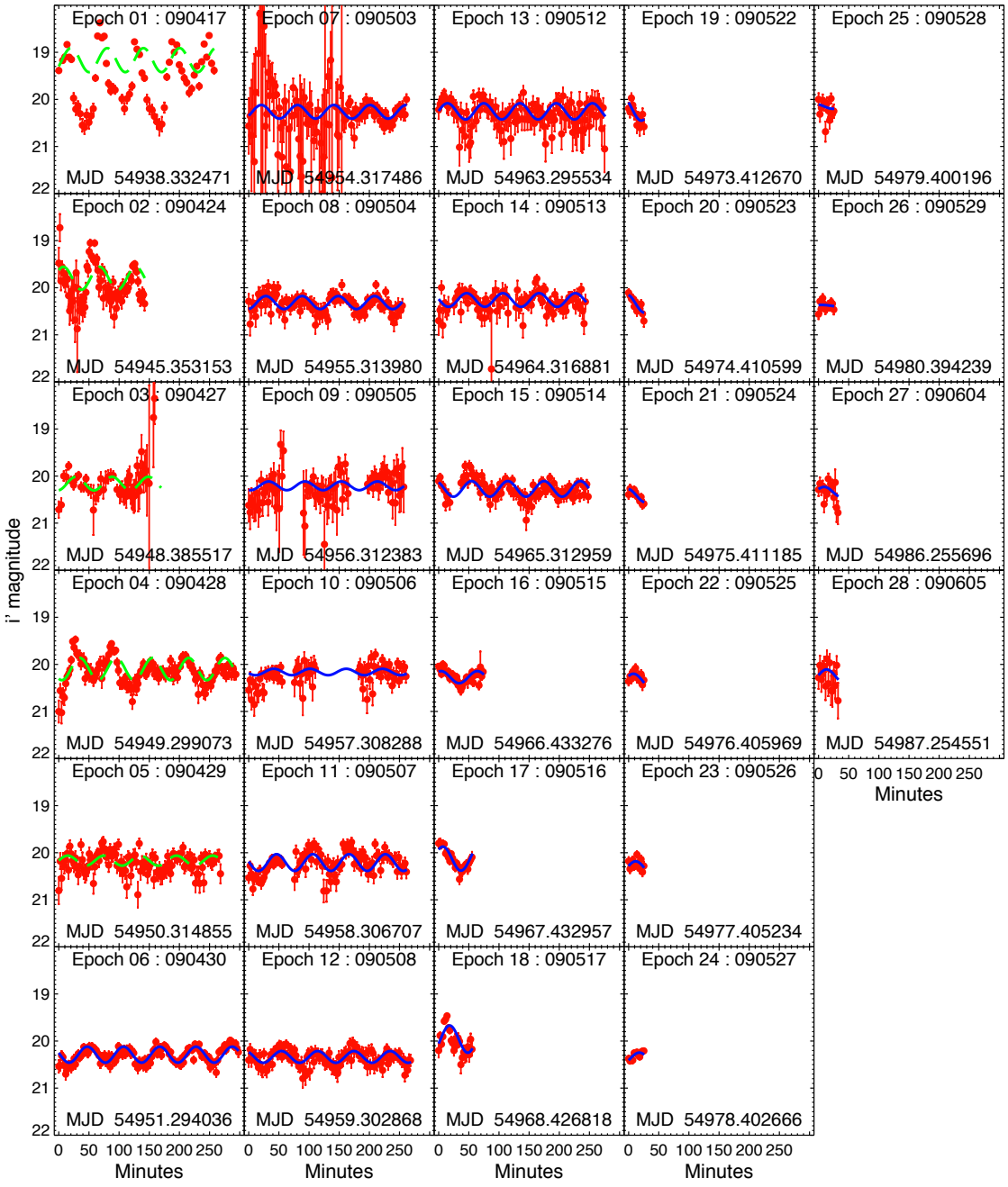

Figure A.3. i' band P60 photometry of 1RXS J1730+03, for Epochs 1 to 28. The source was in outburst in Epoch 1 and slowly faded into quiescence. The error bars denote relative photometry errors and do not include an absolute zero point error of 0.064 mag (§ A.2.1). The solid blue line denotes the best fit sinusoid to the photometric data. The dashed green line is added to show the relative phase of the source in outburst, these epochs were not used for fitting the lightcurve.

from the LFC images to estimate and correct for the extinction by clouds.

A.2.3 X-ray and UV Observations

We observed the 1RXS J1730+03 with the X-ray telescope (XRT) and the UV-Optical Telescope (UVOT) onboard the *Swift* X-ray satellite (Gehrels et al., 2004) during UT 2009 May 3-6 for a total of about 12.5 ks. The level-two event data was processed using *Swift* data analysis threads for the XRT (Photon counting mode; PC) using the `HEASARC FTOOLS` software package. The source was not detected in the X-ray band.

We follow the procedures outlined by Poole et al. (2007) for analyzing the UVOT data. The measured fluxes are given in Table A.3. The contaminator is within the recommended 5″ extraction radius. Hence, flux measurements are upper limits.

Shevchuk et al. (2009) had observed 1RXS J1730+03 on UT 2006 February 9 with the *Swift* satellite as a part of investigations of unidentified ROSAT sources. They detected the source with a count rate of 0.02 counts s^{-} . The best-fit power law has a photon index $\Gamma = 1.8 \pm 0.5$ and a 0.5–10 keV flux of $1.2 \times 10^{-}$ erg cm^{-} s^{-} . After converting to the ROSAT bandpass assuming the XRT model parameters, this value is approximately a factor of two lower than the archival ROSAT flux. They report a much higher UV flux in their observations, which suggests that the source was in an active state during their observations.

The column density inferred from the XRT data is low, $N \sim 7 \times 10$ cm^{-} . From ROSAT data, this column density corresponds to $A = 0.39$, which gives $A = 0.84$ (Cox, 2000). For comparison, Schlegel et al. (1998) give the Galactic dust extinction towards this direction ($l = 26.^{\circ}7$, $b = 19^{\circ}.7$) to be $E(B-V) = 0.141$ mag ($A = 0.44$), corresponding to a column density of about 8×10 cm^{-} .

A.3 Nature Of The Components

The optical spectra (Figure A.6) show rising flux towards the red and blue ends of the spectrum: indicative of a hot (blue) and cool (red) component. The red part of the spectrum shows clear molecular features, characteristic of late type stars. The blue component is

[5] http://heasarc.gsfc.nasa.gov/ftools/; Blackburn (1995)

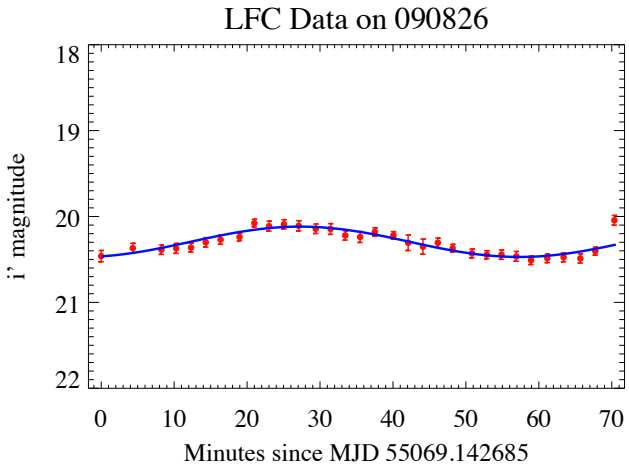

Figure A.4. i' band LFC photometry of 1RXS J1730+03 in quiescence, 131 days after we first saw high variability. The variations have the same phase and period as observed during outburst. See Figure A.3 for details.

devoid of any prominent absorption/emission features. From the overall spectral shape we infer that 1RXS J1730+03 is a CV.

A.3.1 Red Component

The red component of 1RXS J1730+03 is typical of a late type star. In Figure A.8, we compare the red side spectrum of 1RXS J1730+03 with several M-dwarfs. From the shape of the TiO bands at 7053 Å – 7861 Å, we infer that the spectral type to be M3±1. This is consistent with the relatively featureless J band spectrum (McLean et al., 2003). The spectral type indicates an effective temperature of 3400 K (Cox, 2000). The presence of a sodium doublet at 8183/8195 Å implies a luminosity class V.

We also fit the spectrum with model atmospheres calculated by Munari et al. (2005). For late type stars, these models are calculated in steps of $\Delta T = 500$ K, $\Delta \log\ g = 0.5$ and Δ[M/H] = 0.5. We use model atmospheres with no rotational velocity ($V \quad = 0$ km s^{-}) and convolve them with a kernel modeled on the seeing, slit size and pixel size. We ignore the regions contaminated by the telluric A and B bands (7615 Å and 6875 Å). The unknown contribution from the white dwarf was fit as a low order polynomial. We correct for extinction using $A \quad = 0.39$ from X-ray data (Section A.2.3). To measure log g, we use the

Table A.4. Locations of cyclotron harmonics.

Harmonic number	Measured Wavelength (Å)	Measured Frequency (Hz)	Inferred Wavelength (Å)
7	3540	8.4×10	3664
6	4440	6.7×10	4275
5	5180	5.7×10	5130
4	6770	4.4×10	6413
3	8225	3.6×10	8551
2	···	···	12826
1	···	···	25653

[a] B

spectrum in the 8,000 Å – 8,700 Å region, which is expected to have fairly little contamination from the blue component. This region includes the `Ca II` lines at 8498, 8542 Å and the `Na I` doublet, which are sensitive to log g. We then fit the spectra in the 6,700 Å – 8,700 Å range to determine the temperature and metallicity. The best fit model has T = 3500 K, log $g = 5.0$ and solar metallicity, consistent with our determination of the spectral type.

Kolb et al. (2001) state that unevolved donors in CVs follow the spectral type–mass relation of the zero age main sequence, as the effects of thermal disequilibrium on the secondary spectral type are negligible. For a M3 star, this yields a mass of 0.38 $M_{\odot}$. As the secondaries evolve, the spectral type is no longer a good indicator of the mass and gives only an upper limit on the mass. The lower limit can simply be assumed to be the Hydrogen-burning limit of 0.08 $M_{\odot}$.

A.3.2 Blue Component

The blue component of 1RXS J1730+03 is consistent with a highly magnetic white dwarf. The blue spectrum is suggestive of a hot object, but does not show any prominent absorp-

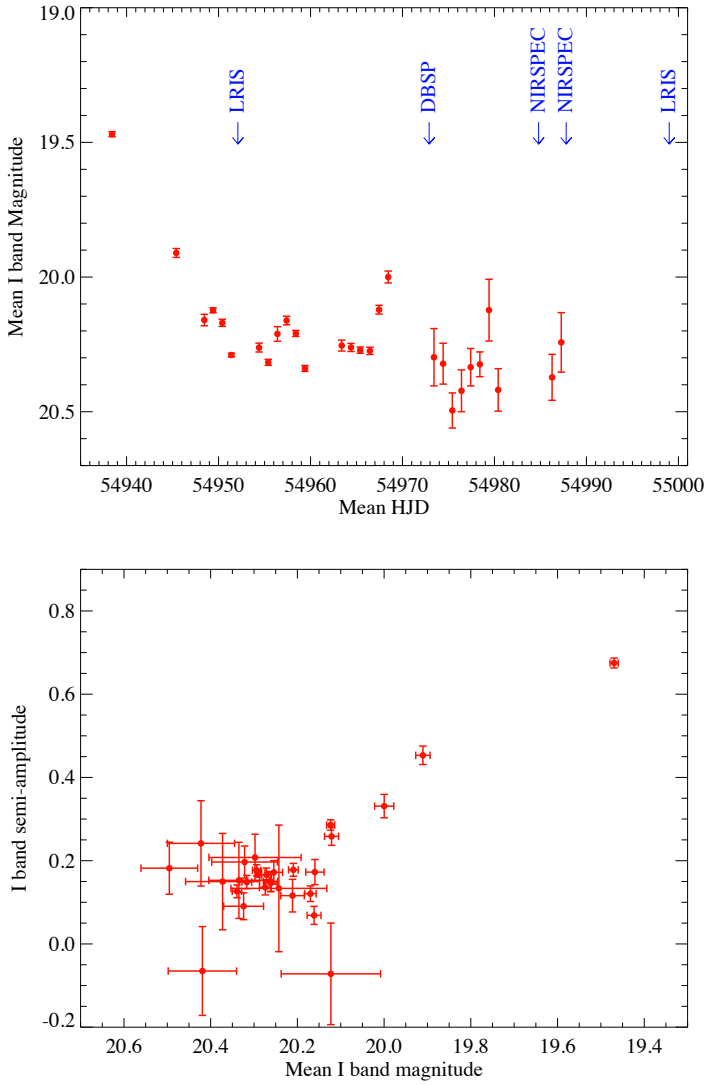

Figure A.5. Photometric evolution of 1RXS J1730+03 in i' band. Data for each epoch was fit with a sinusoid with the same period for all epochs. In contrast to Figures A.3 & A.4, the phase was allowed to vary independently for each epoch. Top: average i' magnitude for each P60 observation epoch, as a function of time. Blue arrows mark spectroscopy epochs. Bottom: semi-amplitude of sinusoidal variations as a function of the corresponding mean i' magnitudes for each epoch.

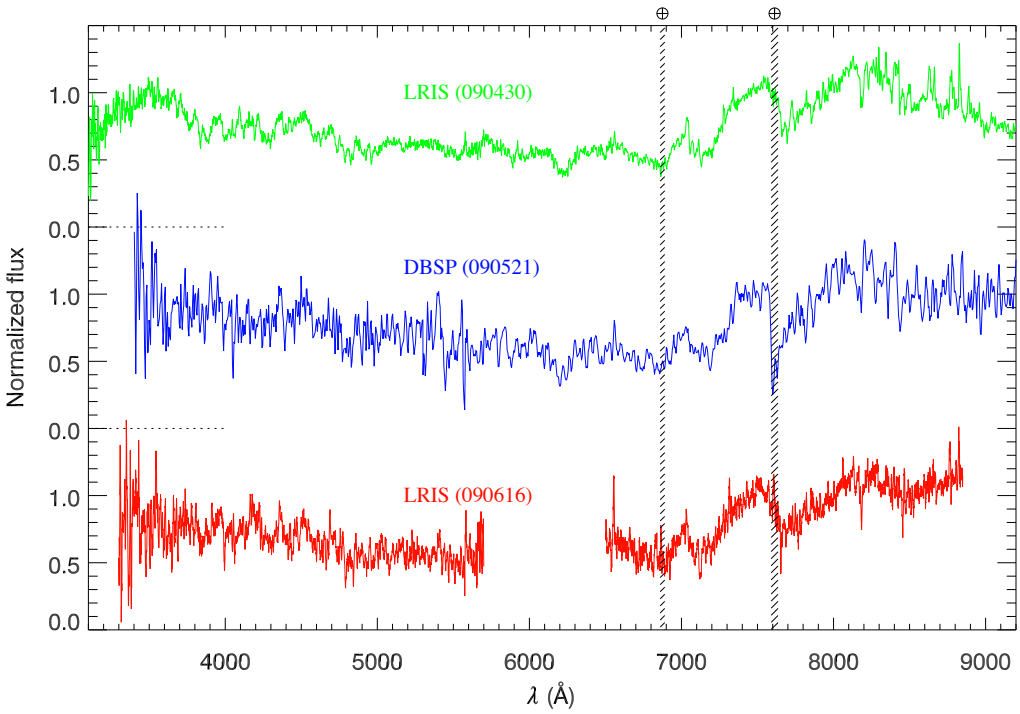

Figure A.6. Temporal evolution of 1RXS J1730+03 spectra. Some spectra are not corrected for Telluric absorption, the affected regions are diagonally hatched. The first spectrum was obtained 13 days after we measured high variability, the second after 34 days, and the lowermost spectrum after 60 days. The spectra show broad Balmer features which evolve with time. The M-dwarf features (TiO, Na I) are clearly seen at all times.

tion/emission features. Hα is seen in emission, but other Balmer features are not detected. The spectrum (Figure A.6) shows cyclotron humps, suggesting the presence of a strong magnetic field. The polar nature of the object is supported by the absence of an accretion disc, and the transition from an active state to an off state in X-rays (Section A.1, Section A.2.3).

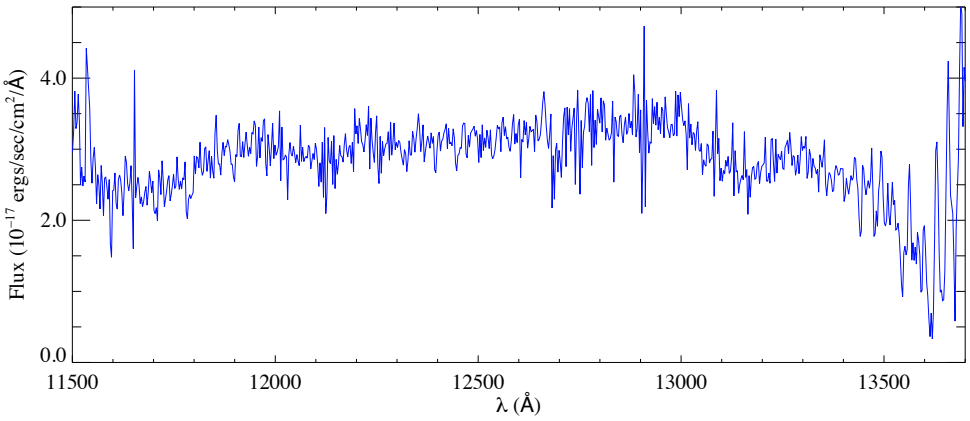

Figure A.7. Keck NIRSPEC spectrum of 1RXS J1730+03. The spectrum is flat and nearly featureless, as expected for early M stars.

For analyzing the WD spectrum, we subtracted a scaled spectrum of the M-dwarf GL 694 from the composite spectrum of 1RXS J1730+03. The resultant spectrum (Figure A.9) clearly shows cyclotron harmonics. The hump seen in the J-band spectrum (Figure A.7) is also inferred to be a cyclotron harmonic. A detailed modeling of the magnetic field is beyond the scope of this work, but we use a simple model to estimate the magnetic field. We fit the cyclotron humps with Gaussians and measure the central wavelengths (Table A.4). We then fit these as a series of harmonics, and infer that the cyclotron frequency is ν $= 1.17 \times 10$ Hz. The magnetic field in the emission region is given by, $B = (\nu$ $/2.8 \times 10$ Hz$) \cdot 10$ G $= 42 \times 10$ G.

As a conservative error estimate, we consider the worst case scenario where our identified locations for the cyclotron humps are off by half the spacing between consecutive cyclotron harmonics. Using this, we estimate the errors on the magnetic field: $B = 42\_$ MG.

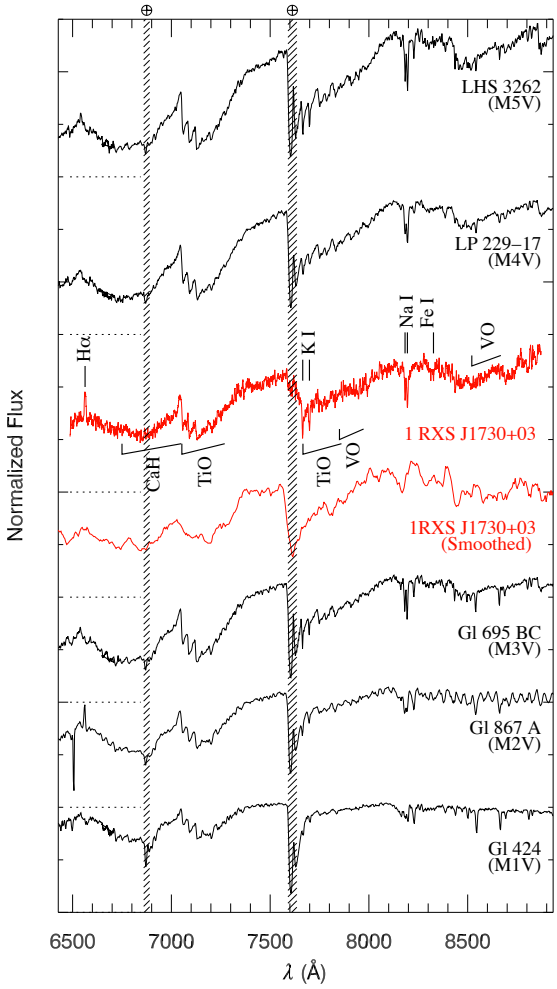

Figure A.8. Comparison of red part of 1RXS J1730+03 spectrum with M-dwarf spectra. Some spectra are not corrected for Telluric absorption, the affected regions are diagonally hatched. Prominent bands (TiO, CaH) and lines (Hα, Na I) are marked. Comparing the shape of the TiO bands at 7053–7861 Å and the shape of the continuum redwards of 8200 Å, we infer that spectral type of the red component to be M3. The presence of a sodium doublet at 8183/8195 Å implies a luminosity class V.

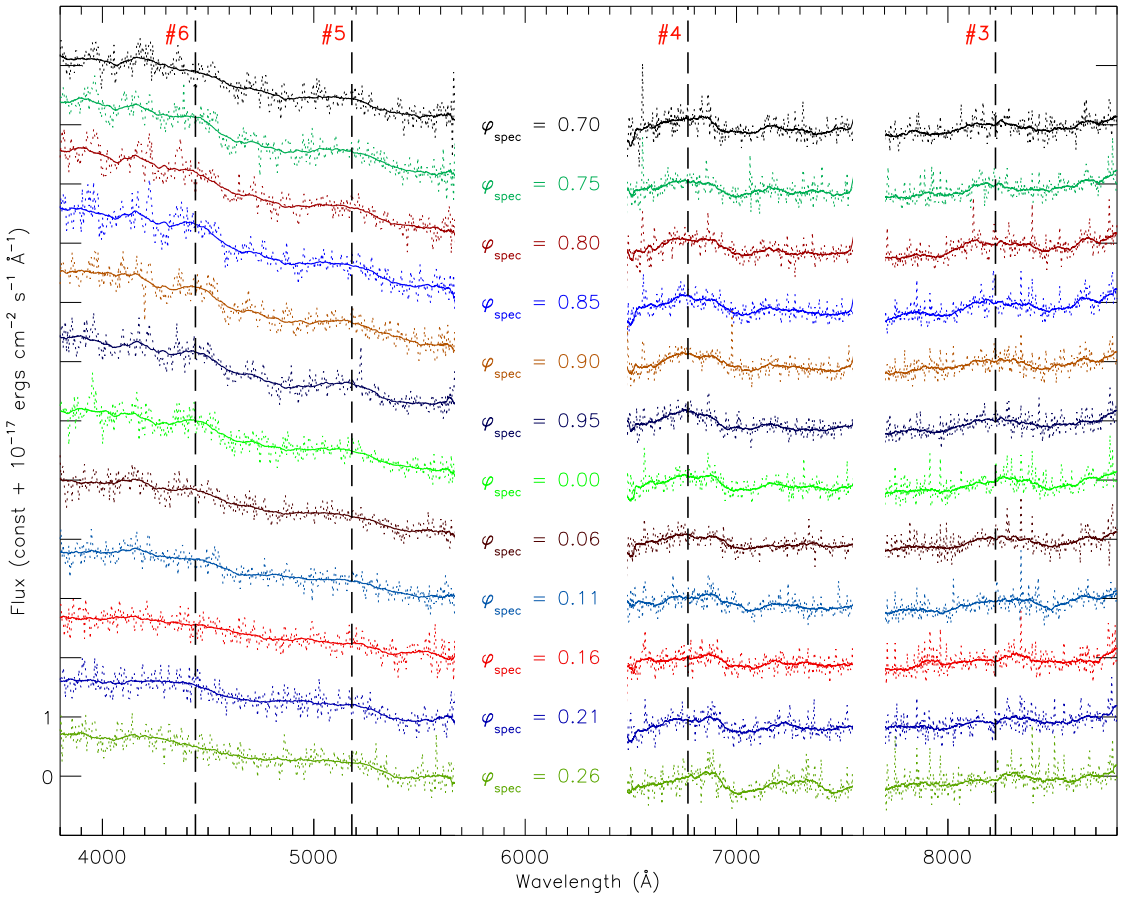

Figure A.9. Blue component spectra of 1RXS J1730+03, showing the 12 late-time LRIS exposures (Section A.2.2, Table A.5). The spectroscopic phase at mid-exposure is indicated for each spectrum. Dotted lines show spectra are obtained by subtracting a scaled spectrum of GL 694 from spectra of this binary. The overlaid solid lines are smoothed versions of the same spectra. Vertical dashed cyclotron humps at 4440 Å, 5180 Å, 6770 Å & 8225 Å. The cyclotron harmonic numbers (#3 – #6) are indicated in bold red. Two more cyclotron humps are seen in other spectra: a feature at 3540 Å (Figure A.6), and a J-band feature (Figure A.7).

A.4 System Parameters

A.4.1 Orbit

We use the best fit Munari et al. (2005) model atmosphere to measure radial velocities of the M-dwarf. We vary the radial velocity of the model, and minimize the χ over the 6,500 Å – 8,700 Å spectral region, excluding the telluric O bands. After a first iteration, the spectra are re-fit to account for motion of the M-dwarf during the integration time. For the 12 spectra taken at the second LRIS epoch, we also measure the radial velocity for the contaminator star on the slit, and find it to be constant. This serves as a useful test for our radial velocity measurement procedure. The barycentric corrected velocities are given in Table A.5.

We fit a circular orbit ($v = \gamma + K \sin([2\pi(t - t)]/P)$) to the measured velocities. We define the superior conjunction of the WD as phase 0.

The 2009 June 16 spectroscopic data (Table A.5) give an orbital period $P = 123 \pm 3$ min. We then use the photometric variability (Section A.4.2) to determine an accurate period in this range. Next, we refine the solution with velocity measurements from the other two spectroscopic epochs. The best-fit solution gives a period $P = 120.2090 \pm 0.0013$ min and $K = 390 \pm 4$ km s^{-} (Table A.6, Figure A.10).

Figure A.11 shows sections of the last epoch spectra around Hα and the `Na I` doublet at 8184/8195 Å. The `Na I` doublet clearly matches the velocity of the M-dwarf in the orbit, but the Hα emission seems to have a smaller velocity amplitude. A possible explanation for this is that the Hα emission comes from the M-dwarf surface that is closest to the WD, which may be heated by emission from the white dwarf or the accretion region.

A.4.2 Photometric Variability

The lightcurve of 1RXS J1730+03 shows clear periodicity (Figures A.2–A.4), with two peaks per spectroscopic period. Most of the photometric data was acquired in the i' band, which contains contribution from both the M-dwarf and a cyclotron harmonic from the emission region near the WD.

A Fourier transform of the data (Figure A.12) shows a strong peak at sixty minutes.

[6] When the WD is furthest from the observer along the line of sight.

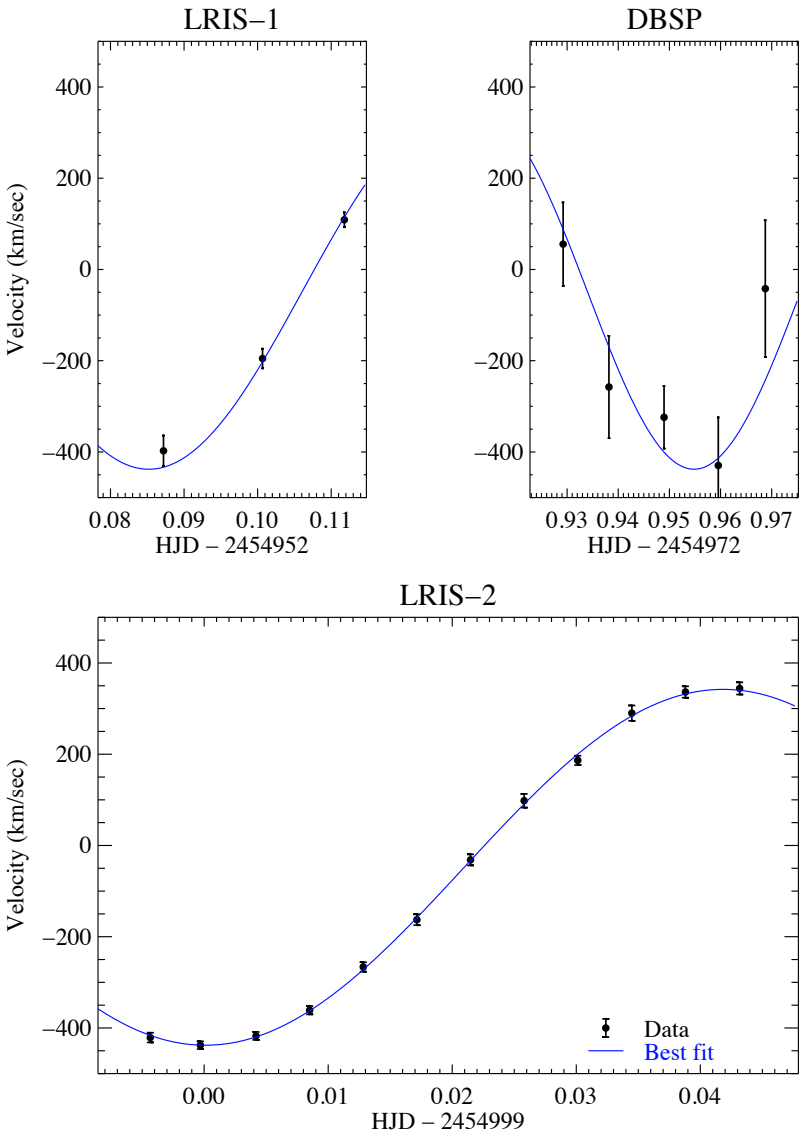

Figure A.10. Velocity measurements 1RXS J1730+03. The best-fit solution gives $P = 120.2090 \pm 0.0013$ min, $\gamma_2 = -48 \pm 5$ km s^{-1} and $K_2 = 390 \pm 4$ km s^{-1} (Section A.4.1)

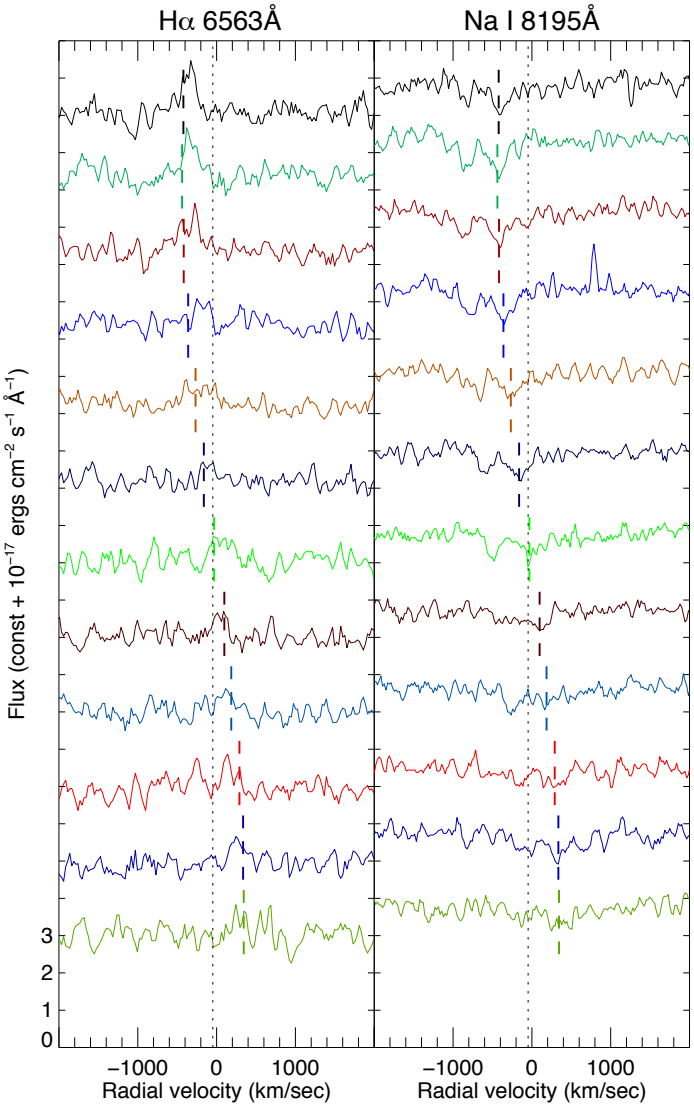

Figure A.11. Velocity modulation of Hα and the 8184/8195 Å `Na I` doublet. The spectra are offset by 2×10^{-17} erg cm^{-2} s^{-1} for clarity. The wavelengths are converted into velocities using the rest wavelengths 6563 Å and 8195 Å respectively. The vertical dotted line marks the radial velocity of the binary barycenter. The short dashed lines mark the radial velocities measured by fitting the complete spectrum. The `Na I` absorption follows the radial velocity of the M-dwarf, but Hα seems to have a smaller velocity amplitude.

Table A.5. Radial velocity of the M-dwarf.

		$^{-1}$	
		$-$ $\pm$	[a]
		$-$ $\pm$	[a]
		$\pm$	[a]
		$\pm$	[b]
		$-$ $\pm$	[b]
		$-$ $\pm$	[b]
		$-$ $\pm$	[b]
		$-$ $\pm$	[b]
		$-$ $\pm$	[c]
		$-$ $\pm$	[c]
		$-$ $\pm$	[c]
		$-$ $\pm$	[c]
		$-$ $\pm$	[c]
		$-$ $\pm$	[c]
		$-$ $\pm$	[c]
		$\pm$	[c]
		$\pm$	[c]
		$\pm$	[c]
		$\pm$	[c]
		$\pm$	[c]

[a]

$^{-1}$

$R \sim$

$^{-1}$ $R \sim$

$''$

[b]

$^{-1}$ $R \sim$

$^{-1}$ $R \sim$

$''$

[c]

$^{-1}$ $R \sim$

$^{-1}$ $R \sim$ $''$

Table A.6. Orbital velocity parameters of the M-dwarf.

Parameter	Value
γ (km s$^-$)	-48 ± 5
K (km s$^-$)	390 ± 4
t (HJD)	54998.9375 ± 0.0003
P (min)	120.2090 ± 0.0013

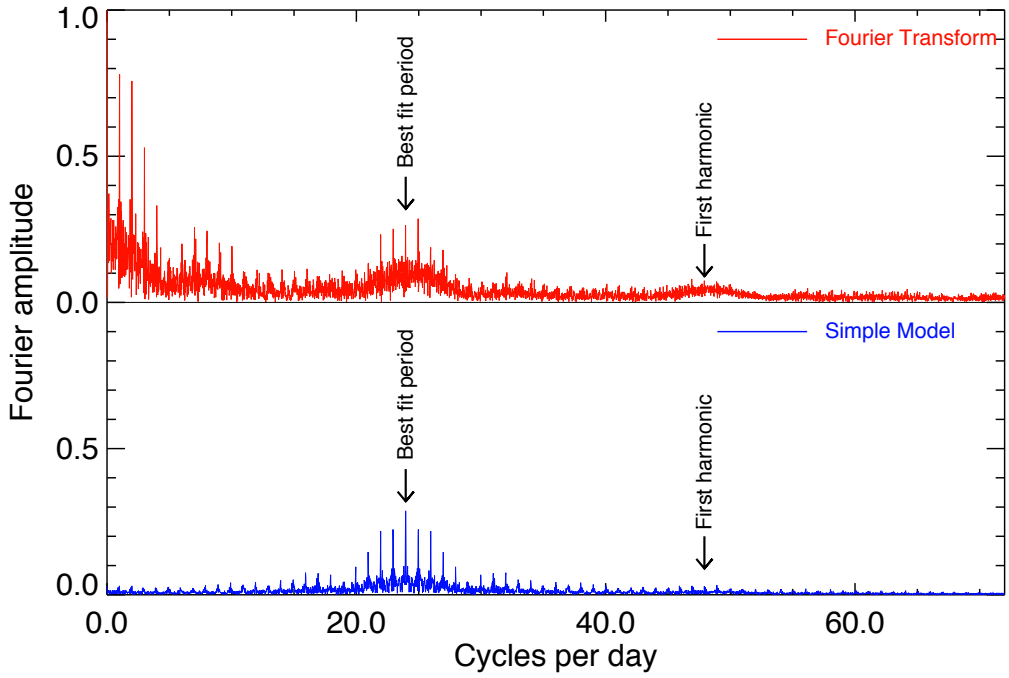

Figure A.12. Upper panel: Fourier transform of all i' data. Lower panel: expected Fourier transform for a pure sinusoidal variations with a period of 60.11 min, obtained by scaling and convolving the Fourier transform of the window function with a delta function corresponding to the best-fit period.

We interpret this as a harmonic of the orbital period. To determine the exact period, we analyze the data as follows. As the object has a short orbital period, we convert all times to Heliocentric Julian Date for analysis. We fit a sinusoid ($m \ + m_A \sin([2\pi(t - t\ )]/P)$) to each epoch, allowing m and m_A to vary independently for each epoch, but we use the same reference time t and period P for the entire fit. The mean magnitude is correlated with the amplitude (Figure A.5). Note that the amplitude measured for the sinusoidal approximation for each epoch is always less than the actual peak-to-peak variations of the source during that epoch, as expected. The source is in the active state in the first few epochs, and we exclude epochs 1 – 5 from the fit, to avoid contamination from the accretion stream and/or the accretion shock.

The best-fit solution is overplotted in blue in Figures A.3 & A.4. Since epochs 1 – 5 were not included in the fit, a sinusoid is overplotted in dashed green to indicate the expected phase of the variations. The best-fit period is 60.1059 ± 0.0005 minutes. This formally differs from the spectroscopically determined orbital period by 2.1σ. However, this error estimate includes only statistical errors. There is some, difficult to determine, systematic error component in addition, so we do not claim any significant inconsistency.

Periodic photometric variability for 1RXS J1730+03 can be explained as a combination of two effects: cyclotron emission from the accretion region and ellipsoidal modulation. The active state is characterized by a higher mass transfer rate from the donor to the WD, and results in higher cyclotron emission. This emission is beamed nearly perpendicular to the magnetic field lines, creating an emission fan beam. For high inclination systems, the observer crosses this fan beam twice, causing two high amplitude peaks per orbit (Figure A.2). In the active state when the emission is dominated by cyclotron radiation, the minimum leads the superior conjuntion by $\sim 47°$.

In ellipsoidal modulation, and the photometric minima coincide with the superior conjunction. It is observed that in quiescence, the photometric minimum leads the superior conjunction of the white dwarf by $\sim 14°$. This suggests that the 0.29 ± 0.13 mag variation is caused by a combination of ellipsoidal modulation and cyclotron emission from the accretion region.

A.4.3 Mass Ratio

The semi-amplitude of the M-dwarf radial velocity, K2, gives a lower limit on the mass of the white dwarf. For a circular orbit, one can derive from Kepler's laws that:

$$M_{,} = \frac{PK}{2\pi G} = 0.52\ M_{\odot} \tag{A.1}$$

Tighter constraints can be placed on the individual component masses $M_{,}$ M by considering the geometry of the system. Eggleton (1983) expresses the volume radius R of the secondary in terms of the mass ratio $q = M_{/}M$:

$$\frac{R}{a} = \frac{0.49q^{/}}{0.6q^{/} + \ln(1+q^{/})} \tag{A.2}$$

where the separation of the components is given by $a = [P\ G(M + M)/4\pi]^{/}$. Thus for a fixed period P, R depends only on M . The radius of the white dwarf is much smaller than that of the M-dwarf. Hence, the M-dwarf will eclipse the accretion region if the inclination of the system is $i < \sin^{-}(R/a)$. Figures A.3, A.4 show that we do not detect any eclipses in the system.

Figure A.13 shows the allowed region for 1RXS J1730+03 in a WD mass–M-dwarf mass phase space. The orange dotted region is excluded as the orbital velocity would be greater than the measured projected velocity. The red hatched region is excluded by non-detection of eclipses. The allowed mass of the primary ranges from the minimum mass ($M > 0.52\ M_{\odot}$) to the Chandrashekhar limit. The mass of the secondary is bounded above by the ZAMS mass for a M3 dwarf ($M = 0.38\ M_{\odot}$).

For a given M and a known orbital period, we can determine the radius of the secondary using Equation (A.2), and can calculate the surface gravity ($\log g$). For $0.38\ M_{\odot} \gtrsim M \gtrsim 0.05\ M_{\odot}$, $\log g$ ranges from 5.1 to 4.8. This is consistent with $\log g = 5.0$ for the best fit M-dwarf spectrum (Section A.3.1).

The donor stars in CVs are expected to co-rotate. For 1RXS J1730+03, the highest possible rotational velocity $v \sin i$ is $\sim$ 160 km s^{-} for a 0.38 $M_{\odot}$, 0.27 $R_{\odot}$ M-dwarf and a 1.1 $M_{\odot}$ WD (Figure A.13). $v \sin i$ will be lower if the WD is heavier or if the M-dwarf is lighter. To measure rotational broadening in the spectra, we use a higher resolution ($R = 20,000$) template of the best-fit model from Zwitter et al. (2004). We take a tem-

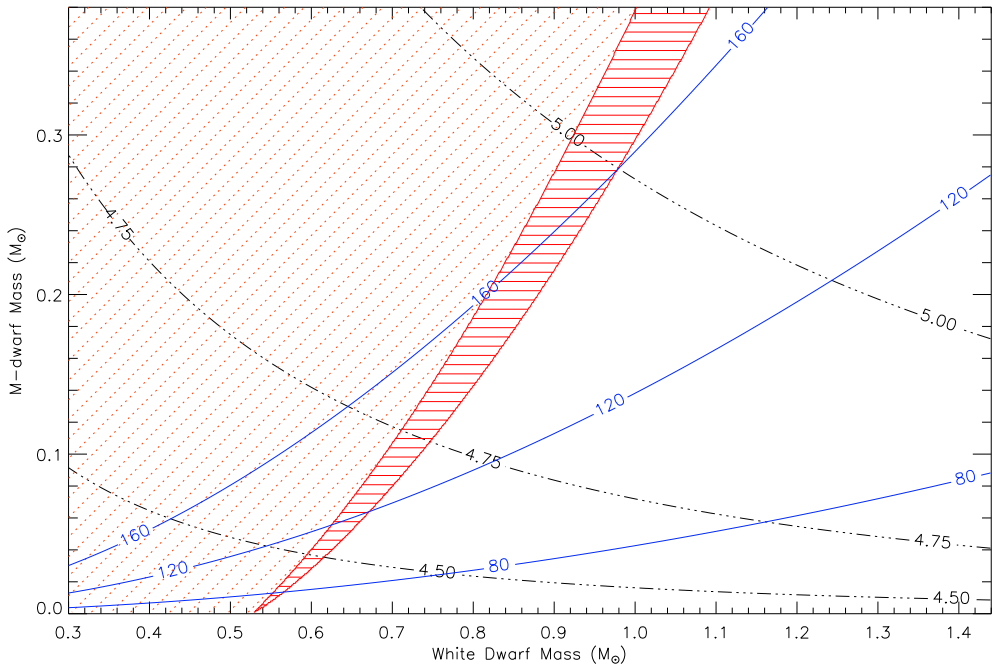

Figure A.13. The allowed range of masses (clear white region) for components of 1RXS J1730+03. The orange dotted region is excluded by the minimum inferred masses from radial velocity measurements. The red hashed region is excluded by non-detection of eclipses (Figures A.3, A.4). The black dash-dot lines show contours of constant log g. The best fit spectra yeild log $g = 5.0$. The solid blue lines are calculated contours for the rotation velocity (km s^{-1}) of the M-dwarf. A measurement of $v \sin i$ will help to constrain masses of the components.

plate with zero rotation velocity and broaden it to different rotational velocities using the prescription by Gray (2005). Then we use our fitting procedure (Section A.3.1) to find the best-fit value for $v \sin i$. For this measurement, we use only the 12 relatively high resolution spectra from the second LRIS epoch (UT 2009 June 16). The weighted $v \sin i$ from the twelve spectra is 97 ± 22 km s^{-} , but the measurements show high scatter, with a standard deviation of 54 km s^{-} . We compared our broadened spectra with rotationally broadened spectra computed by Zwitter et al. (2004), and found that our methods systematically underestimate $v \sin i$ by $\sim$ 20 km s^{-} . We do not understand the reason for this discrepancy, hence do not feel confident enough to use this value in our analysis. A reliable measurement of $v \sin i$ will help better constrain the masses of the two components.

A.4.4 Distance

We estimate the distance to 1RXS J1730+03 as follows. Our fitting procedure (Section A.3.1) corrects for extinction and separates the WD and M-dwarf components of the spectra. We correct for varying sky conditions by using a reference star on the slit. The ratio of measured flux to the flux of the best fit model atmosphere ($T = 3500$ K, $\log g = 5.0$) is,

$$\frac{f}{f} = \left(\frac{R}{d}\right) = (6.1 \pm 1.6) \times 10^{-} \tag{A.3}$$

where d is the distance to the source, and R is given by Equation (A.2).

For 1RXS J1730+03, the maximum mass of the M-dwarf is 0.38 $M_{\odot}$, and the corresponding radius is $R = 0.27\ R_{\odot}$. Equation (A.3) then gives $d = 800 \pm 110$ pc. This calculation assumes the largest possible M-dwarf radius, hence is an upper limit to distance. If the M-dwarf is lighter, say 0.1 $M_{\odot}$, we get $R = 0.17\ R_{\odot}$, yielding $d = 500 \pm 70$ pc.

A.5 Conclusion

1RXS J173006.4+033813 is a polar cataclysmic variable, similar to known well-studied systems like BL Hyi, ST LMi and WW Hor in terms of the orbital period, magnetic field and variability between active and quiescent states. This source is notable for the highly symmetric nature and high amplitude of the double–peaked variation in the active state. This suggests a relatively high angle between the rotation and magnetic axes. Polarimetric

observations of the source would help to better constrain the magnetic field geometry of the system.

Most polars are discovered due to their highly variable X-ray flux. However, we mounted a followup campaign for 1RXS J1730+03 due to its unusual optical variability properties. This suggests that current and future optical synoptic surveys, such as PTF [7] (Law et al., 2009) and LSST can uncover a large sample of polars by cross-correlating opticaly variable objects with the ROSAT catalog.

Acknowledgements

We sincerely thank the anonymous referee for detailed comments on the paper. We thank N. Gehrels for approving the Target of Opportunity observation with *Swift*, and the *Swift* team for executing the observation. We also thank V. Anupama, L. Bildsten, T. Marsh, G. Nelemans, E. Ofek and P. Szkody and for useful discussions while writing the paper.

This research has benefitted from the M, L, and T dwarf compendium housed at `DwarfArchives.org` and maintained by Chris Gelino, Davy Kirkpatrick, and Adam Burgasser.

Some of the data presented herein were obtained at the W.M. Keck Observatory, which is operated as a scientific partnership among the California Institute of Technology, the University of California and the National Aeronautics and Space Administration. The Observatory was made possible by the generous financial support of the W.M. Keck Foundation.

Facilities: PO:1.5m. Hale (LFC, DBSP), Keck:I (LRIS), Keck:II (NIRSPEC), Swift

[7] http://www.astro.caltech.edu/ptf

Appendix B

Transformation of a Star into a Planet in a Millisecond Pulsar Binary

M. Bailes[a,b,c,] , S. D. Bates[d] , V. Bhalerao[e], N. D. R. Bhat[a,c], M. Burgay[f], S. Burke-Spolaor[g], N. D'Amico[f,i], S. Johnston[g], M. J. Keith[g], M. Kramer[h,d], S. R. Kulkarni[e], L. Levin[a,g], A. G. Lyne[d], S. Milia[i,f], A. Possenti[f], L. Spitler[a], B. Stappers[d], W. van Straten[a,c]

[a]Centre for Astrophysics and Supercomputing, Swinburne University of Technology, PO Box 218 Hawthorn, VIC 3122, Australia.

[b]Department of Astronomy, University of California, Berkeley, CA, 94720, USA.

[c]ARC Centre for All-Sky Astronomy (CAASTRO).

[d]Jodrell Bank Centre for Astrophysics, School of Physics and Astronomy, The University of Manchester, Manchester M13 9PL, UK.

[e]Caltech Optical Observatories, California Institute of Technology, MS 249-17, Pasadena, CA 91125, USA.

[f]INAF - Osservatorio Astronomico di Cagliari, Poggio dei Pini, 09012 Capoterra, Italy.

[g]Australia Telescope National Facility, CSIRO Astronomy and Space Science, P.O. Box 76, Epping NSW 1710, Australia.

[h]MPI fuer Radioastronomie, Auf dem Huegel 69, 53121 Bonn, Germany.

[i]Dipartimento di Fisica, Università degli Studi di Cagliari, Cittadella Universitaria, 09042 Monserrato (CA), Italy.

A version of this chapter was first published in *Science* (Bailes et al., 2011). It is reproduced here as per the licensing policy of AAAS, http://www.sciencemag.org/feature/contribinfo/prep/lic_info.pdf, Retreived May 6, 2012. My role was restricted to optical observations and data analysis of the counterpart.

[1]To whom correspondence should be addressed. Email: mbailes@swin.edu.au

Millisecond pulsars are thought to be neutron stars that have been spun-up by accretion of matter from a binary companion. Although most are in binary systems, some 30% are solitary, and their origin is therefore mysterious. PSR J1719−1438, a 5.7 ms pulsar, was detected in a recent survey with the Parkes 64 m radio telescope. We show that it is in a binary system with an orbital period of 2.2 h. Its companion's mass is near that of Jupiter, but its minimum density of 23 g cm^{-} suggests that it may be an ultra-low mass carbon white dwarf. This system may thus have once been an Ultra Compact Low-Mass X-ray Binary, where the companion narrowly avoided complete destruction.

Radio pulsars are commonly accepted to be neutron stars that are produced in the supernova explosions of their progenitor stars. They are thought to be born with rapid rotation speeds (∼50 Hz) but within a few 100,000 yr slow to longer periods because of the braking torque induced by their high magnetic field strengths (∼10 G). By the time their rotation periods have reached a few seconds the majority have ceased to radiate at radio wavelengths. The overwhelming majority (∼ 99%) of slow radio pulsars are solitary objects. In contrast ∼ 70% of the millisecond pulsars (MSPs) are members of binary systems and possess spin frequencies of up to 716 Hz (Hessels et al., 2006). This is consistent with the standard model for their origin in which an otherwise dead pulsar is spun-up by the accretion of matter from a companion star as it expands at the end of its life (Bhattacharya & van den Heuvel, 1991). Through some process yet to be fully understood, the recycling not only spins up the neutron star but leads to a large reduction of the star's magnetic field strength to $B \sim 10$ G and usually leaves behind a white dwarf companion of typically 0.2-0.5 $M_{\odot}$. The lack of a compelling model for this reduction of the magnetic field strength with continuing mass accretion, and issues between the birthrates of MSPs and their putative progenitors, the low-mass X-ray binaries (LMXBs) led to an early suggestion (Grindlay & Bailyn, 1988) that accretion induced collapse of a white dwarf might form MSPs "directly" in the cores of globular clusters, and possibly in the Galactic disk.

In the standard model, the reason why some MSPs possess white dwarf companions and others are solitary is unclear. Originally it was proposed that solitary MSPs might be

formed from a different channel, in which a massive ($M > 0.7$ M$_\odot$) white dwarf coalesces with a neutron star (van den Heuvel & Bonsdema, 1984). The binary pulsar-white dwarf system PSR J1141−6545 (Kaspi et al., 2000) is destined to merge in < 2 Gyr and thus is a potential progenitor for this scenario. At lower white dwarf masses, the final product is less clear, as the mass transfer can stabilise (Bonsema & van den Heuvel, 1985). From an observational point of view, the "black widow" MSPs may give some insights. In these systems an MSP is usually accompanied by a low-mass $\sim$ 0.02-0.05 M$_\odot$ companion in close orbits of a few hours. It was initially believed these systems might evaporate what was left of the donor star (Fruchter et al., 1988), but other examples (Stappers et al., 1998) meant that the timescales were too long.

The MSP population was further complicated by the detection of an extra-solar planetary system in orbit around the fifth MSP found in the Galactic disk, PSR B1257+12 (Wolszczan & Frail, 1992). This system has two $\sim$3 Earth-mass planets in 67- and 98-day orbits, and a smaller body of lunar mass in a 25 d orbit. The planets were probably formed from a disk of material. The origin of this disk is however the subject of much speculation, ranging from some catastrophic event in the binary that may have recycled the pulsar (Wijers et al., 1992) to ablation (Rasio et al., 1992) and supernova fall-back (Hansen et al., 2009). A large number of potential models for the creation of this system have been proposed, and are summarised in the review by Podsiadlowski (1993). Although more than another 60 MSPs ($P < 20$ ms) have been detected in the Galactic disk since PSR B1257+12, until now none have possessed planetary-mass companions.

PSR J1719−1438 was discovered in the High Time Resolution Universe survey for pulsars and fast transients (Keith et al., 2010). This $P = 5.7$ ms pulsar was also detected in archival data from the Swinburne intermediate latitude pulsar survey (Edwards et al., 2001). Its mean 20 cm flux density is just 0.2 mJy but at the time of discovery was closer to 0.7 mJy due to the effects of interstellar scintillation. We soon commenced regular timing of the pulsar with the Lovell 76-m telescope that soon revealed that the pulsar was a member of a binary with an orbital period of 2.17 h and a projected semi-major axis of just $a \sin i$=1.82 ms (Figure B.1). Since then we have performed regular timing of the pulsar at the Parkes and Lovell telescopes that have enabled a phase-coherent timing solution over a one year period. There is no evidence for any statistically significant orbital eccentricity

with a formal 2-σ limit of $e < 0.06$.

With these observations, we can explore the allowed range of companion masses from the binary mass function that relates the companion mass m , orbital inclination angle i and pulsar mass m to the observed projected pulsar semi-major axis a , orbital period P and gravitational constant G:

$$f(m_c) = \frac{4\pi}{G}\frac{(a \sin i)}{P} = \frac{(m_c \sin i)}{(m_c + m_p)} = 7.85(1) \times 10^{-} \quad M_{\odot} \tag{B.1}$$

Only a few MSPs in the Galactic disk have accurate masses (Jacoby et al., 2005; Verbiest et al., 2008; Demorest et al., 2010), and these range from 1.4–2.0 $M_{\odot}$. Assuming an edge-on orbit ($\sin i = 1$) and pulsar mass $m = 1.4$ $M_{\odot}$ $m > 1.15 \times 10^{-}$ $M_{\odot}$, ie approximately the mass of Jupiter.

We can accurately determine the component separation ($a = a + a$) for the PSR J1719–1438 binary given the observed range of MSP masses using Kepler's third law and because, $m \ll m$, to a high degree of accuracy,

$$a = 0.95 R_{\odot} \left(\frac{m}{1.4\ M_{\odot}}\right)^{/} \tag{B.2}$$

making it one of the most compact radio pulsar binaries. For large mass ratios, the Roche Lobe radius of the companion (Paczynski, 1971) is well approximated by

$$R = 0.462 a \left(\frac{m}{m + m}\right)^{/} \tag{B.3}$$

and dictates the maximum dimension of the companion star. For $i = 90^o$ and a 1.4 $M_{\odot}$ neutron star, the minimum $R = 2.8 \times 10$ km, just 40% of that of Jupiter. On the other hand, for a pulsar mass $m = 2$ $M_{\odot}$, and $i = 18^o$ (the chance probability of $i > 18^o$ is $\sim$95%), then $R = 4.2 \times 10$ km.

A lower limit on the density ρ (the so-called mean density-orbital period relation, Frank et al., 1985) can be derived by combining the above equations.

$$\rho = \frac{3\pi}{0.462\ GP} = 23 \text{ g cm}^{-} \tag{B.4}$$

This density is independent of the inclination angle and the pulsar mass and far in excess

of that of Jupiter or the other gaseous giant planets whose densities are < 2 g cm^{-} .

The mass, radius and hence the nature of the companion of PSR J1719−1438 are critically dependent upon the unknown angle of orbital inclination. After PSR J1719−1438, PSR J2241−5236 (Keith et al., 2011) has the smallest mass function of the other binary pulsars in the Galactic disk, albeit 1000 times larger (Figure B.2). The sin i-dependence of the mass function could mean that PSR J1719−1438 is a physically similar system, but just viewed face-on. This would require an inclination angle of just $i = 5.7^{o}$, for which the chance probability is 0.5%. The only binary pulsar with a similar orbital and spin period is PSR J2051−0827, but the inclination angle required for mass function equivalence in this case has a chance probability of only 0.1%. Of course, as the known population of black widow systems increases, we will eventually observe examples of face-on binaries that mimic those with planetary-mass companions. The current distribution of mass functions among the known population is such that this is still unlikely.

If the pulsar were energetic and the orbit edge-on, we might hope to detect orbital modulation of the companion's light curve in the optical because the pulsar heats the near-side. Our pulsar timing indicates the pulsar's observed frequency derivative $\dot{\nu}$ is $-2.2(2)\times10^{-}$ s^{-} , not atypical of MSPs. However $\dot{\nu}$ is only an upper limit on the intrinsic frequency derivative (Camilo et al., 1994) ($\dot{\nu}$), which is related to the pulsar's distance d and transverse velocity V by the Shklovskii relation.

$$\dot{\nu} = \dot{\nu} \; - \nu V \; /(dc) \tag{B.5}$$

MSPs have relatively high velocities (Toscano et al., 1999) of 50-200 km s^{-} . At the nominal distance of the pulsar from its dispersion measure (1.2 kpc; Cordes & Lazio, 2002) it would take an MSP transverse velocity of only 100 km s^{-} for almost all of the observed $\dot{\nu}$ to be caused by the proper motion of the pulsar.

In the case of negligible proper motion, we can derive the most optimistic impact of the pulsar's radiation for optical detectability by assuming isotropic pulsar emission, a companion albedo of unity, that the companion is a blackbody, and that the orbit is edge-on, thus maximising the illuminated region of the companion. The spin-down energy of a pulsar is $\dot{E} = -4\pi \; I\nu\dot{\nu}$, where I is the moment of inertia of a neutron star and ν is the spin frequency. We find a maximum effective temperature of 4500 K and a peak R-

band magnitude of 26−28, depending upon the assumed 1.2(3) kpc distance to the pulsar (Cordes & Lazio, 2002) and the unknown radius of the companion, which we assume is close to the Roche Lobe radius.

We observed the field surrounding PSR J1719−1438 with the Keck 10-m telescope in the g, R and I bands using the LRIS instrument. If the binary was a face-on analogue of PSR J2051−0827 we might expect to see a star at the location of the pulsar because the R-band magnitude of the binary pulsar companion in the PSR J2051−0827 system is $R \sim$22.5 (Stappers et al., 1999) and it is at a similar distance d from the Sun. The spin-down luminosity of PSR J1719−1438 is however only 0.4 $L_{\odot}$ which is about 30% of that of PSR J2051−0827, and a face-on orbit would mean only half of the bright side of the companion was ever visible. This would mean the expected R-band magnitude would be reduced to $R \sim 24.5$, however at the position of the pulsar there is no visible companion down to a 3-sigma limiting magnitude of R=25.4 (1250s), g=24.1 (1000s) and I=22.5 (1000s) at the anticipated maximum light, where the values in parentheses indicate the integration times (Figure B.3). The magnitude limit would appear to reduce the probability that PSR J1719−1438 is an extremely face-on analogue of PSR J2051–0827, with the caveat that the assumed spin-down energy of the pulsar is still an upper limit because of Equation B.5.

We now consider the more statistically likely possibility that the orbit is nearly edge-on. In this case the relative velocity of the two constituents is > 500 km s^{-} and could potentially lead to a solid-body eclipse for 60 s or so, or if the companion was being ablated we might see excess dispersive delays at orbital phase 0.25 when the pulsar is on the far side of the companion at superior conjunction. Ordinarily the 20 cm mean flux density of 0.2 mJy would make these effects difficult to detect, but a bright scintillation band occurred during one of our long integrations on the source, increasing the flux density sufficiently for us to assert that there are no excess delays or solid-body eclipses occurring in the system (Figure B.1). The extremely small dimension of the Roche lobe of the companion only precludes inclination angles of $i > 87^{o}$. Inspection of Figure B.2 shows that it is completely impossible to fit a hydrogen-rich planet such as Jupiter into the Roche Lobe of the planetary-mass companion. Although difficult, He white dwarfs might just fit if the computational models (Deloye & Bildsten, 2003) are slighty in error ($\sim$ 10%), or the orbit is moderately face on. A carbon white dwarf on the other hand can easily fit inside the Roche Lobe for

any assumed inclination angle. We thus conclude that the companion star(planet) is likely to be the remains of the degenerate core of the star that recycled the pulsar, and probably comprised of He or heavier elements such as carbon.

In the standard model, this MSP would have been spun-up by the transfer of matter from a nearby companion star to near its current period. The UC LMXBs such as XTE J0929−314 (Galloway et al., 2002) are good potential progenitors of PSR J1719−1438. These systems have orbital periods of tens of minutes and higher ($\sim 10\times$) companion masses. They have also been found to exhibit Ne and O lines in their spectra (Juett et al., 2001), suggesting that their companions are not He white dwarfs. Importantly, their spin periods are comparable to that of PSR J1719−1438. As matter is transferred from the degenerate companions to the neutron star, the orbits widen and the radius of the white dwarf expands due to the inverse mass-radius relationship for degenerate objects. Deloye & Bildsten (2003) predicted how the known UC LMXBs would evolve in the future. They demonstrated that the UC LMXB companions could be comprised of either He or Carbon white dwarfs and after 5-10 Gyr might be expected to end up as binary pulsars with orbital periods of ∼1.5h.

If PSR J1719−1438 was once a UC LMXB, mass transfer would have ceased when the radius of the white dwarf became less than that of the Roche Lobe due to mass loss and out-spiral. In the models by Deloye and Bildsten, the He white dwarfs deviate from the $M^{-1/3}$ law very near to the Roche Lobe radius and approximate mass of our companion star for an edge-on orbit. On the other hand, another mass-radius relationship for Carbon white dwarfs of very low mass (Lai et al., 1991) suggests that it is Carbon white dwarfs that have $dR/dM \sim 0$ near $M = 0.0025\mathrm{M}_{\odot}$ (Figure B.2). It thus seems difficult to unambiguously determine the nature of the pulsar companion, but a scenario in which PSR J1719−1438 evolved from a Carbon white dwarf in an UC LMXB has many attractive features. It explains the compact nature of the companion, the spin period of the pulsar and the longer orbital period due to spiral out as a consequence of the mass transfer that spun-up the pulsar. PSR J1719−1438 might therefore be the descendent of an UC LMXB.

However, the question still remains: why are some MSPs solitary while others retain white dwarf companions, and some, like PSR J1719−1438 have exotic companions of planetary mass that are possibly carbon rich? We suggest that the ultimate fate of the binary is determined by the mass and orbital period of the donor star at the time of mass

transfer. Giants with evolved cores that feed the neutron star at a safe (d >few $R_\odot$) distance leave behind white dwarfs of varying mass in circular orbits, with a tendency for the heavier white dwarfs to be accompanied by pulsars with longer pulsar spin periods (P >10 ms). Close systems that transfer matter before a substantial core has formed might be responsible for the black-widow MSPs. A subset of the LMXBs are driven by gravitational radiation losses, and form the ultra-compact systems during a second stage of mass transfer. Their fate is determined by their white dwarf mass and chemical composition at the beginning of this phase. High mass white dwarfs do not overflow their Roche Lobes until they are very close to the neutron star with orbital periods of a few minutes. If the orbit cannot widen fast enough to stop runaway mass transfer we will be left with a solitary MSP or possibly an MSP with a disk that subsequently forms a planetary system. Low mass white dwarf donors transfer matter at longer orbital periods and naturally cease Roche Lobe overflow near the current orbital period and implied mass of the companion of PSR J1719−1438. The rarity of MSPs with planetary-mass companions means that the production of planets is the exception rather than the rule, and requires special circumstances, like some unusual combination of white dwarf mass and chemical composition.

PSR J1719−1438 demonstrates that special circumstances can conspire during binary pulsar evolution that allows neutron star stellar companions to be transformed into exotic planets unlike those likely to be found anywhere else in the Universe. The chemical composition, pressure and dimensions of the companion make it certain to be crystallized (ie diamond).

Parameter	Value
Right Ascension (J2000) (hh:mm:ss)	17:19:10.0730(1)
Declination (J2000) (dd:mm:ss)	−14:38:00.96(2)
ν (s^{-})	172.70704459860(3) Hz
$\dot{\nu}$ (s^{-})	–2.2(2)×10^{-}
Period Epoch (MJD)	55411.0
DM (pc cm^{-})	36.766(2)
P (d)	0.090706293(2)
$a \sin i$ (lt-s)	0.001819(1)
T (MJD)	55235.51652439
e	< 0.06
Data Span (MJD)	55236-55586
Weighted RMS residual (μs)	15
Points in fit	343
Mean 0.73 GHz Flux Density (mJy)	0.8*
Mean 1.4 GHz Flux Density (mJy)	0.2
Derived parameters	
Characteristic Age (Gyr)	>12.5
B (G)	<2×10
Dispersion Measure Distance (kpc)	1.2 (3)
Spin-down Luminosity L$_{\odot}$	<0.40(4)

* Derived from a single observation.

Note. Differencing of two summed images at the expected maximum and minimum light of the companion also failed to reveal any modulation of flux from any potential candidates near the nominal pulsar position.

Acknowledgements.

The Parkes Observatory is part of the Australia Telescope which is funded by the Commonwealth of Australia for operation as a National Facility managed by CSIRO. This project is supported by the ARC Programmes under grants DP0985270, DP1094370 & CE110001020. Access to the Lovell telescope is funded through an STFC rolling grant. Keck telescope time is made available through a special collaborative program between

Swinburne University of Technology and Caltech. We are grateful to J Roy and Y Gupta for early attempts to obtain a pulsar position with the GMRT.

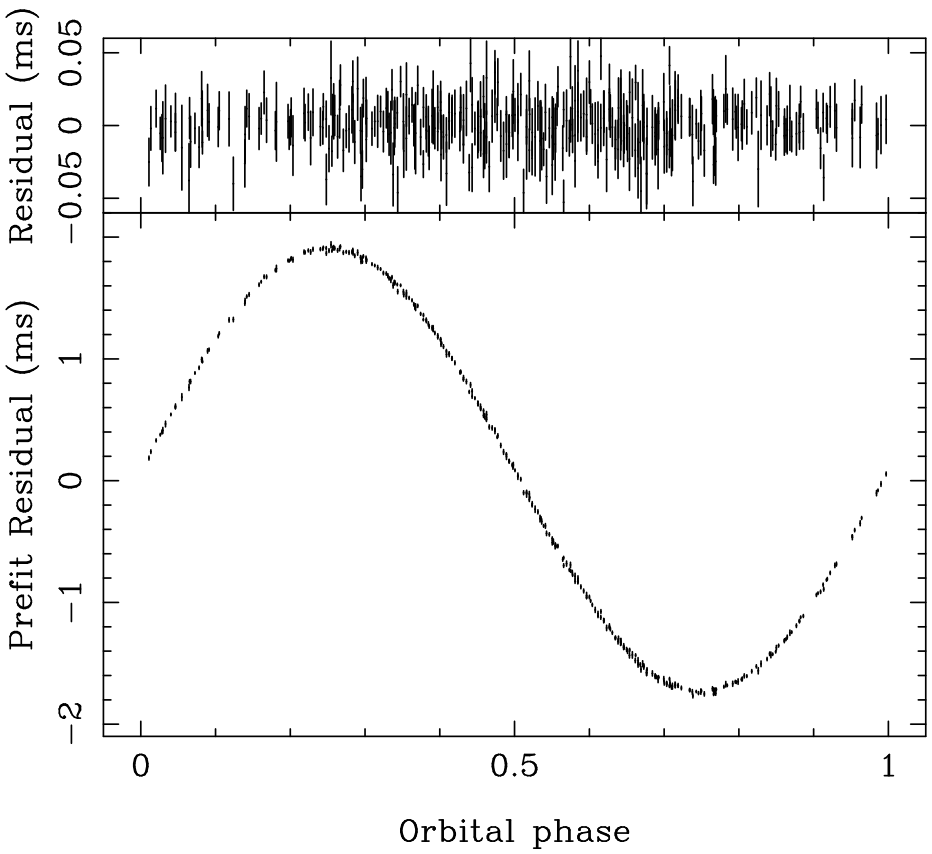

Figure B.1. Upper panel: Pulse timing residuals for PSR J1719−1438 as a function of orbital phase using the ephemeris in Table 1. Lower panel: Residuals after setting the semi-major axis to zero to demonstrate the effect of the binary motion. There is no significant orbital eccentricity. At superior conjunction (orbital phase 0.25) there is no evidence for solid-body eclipses or excess dispersive delays. The arrival times and ephemeris are provided in the supporting online material.

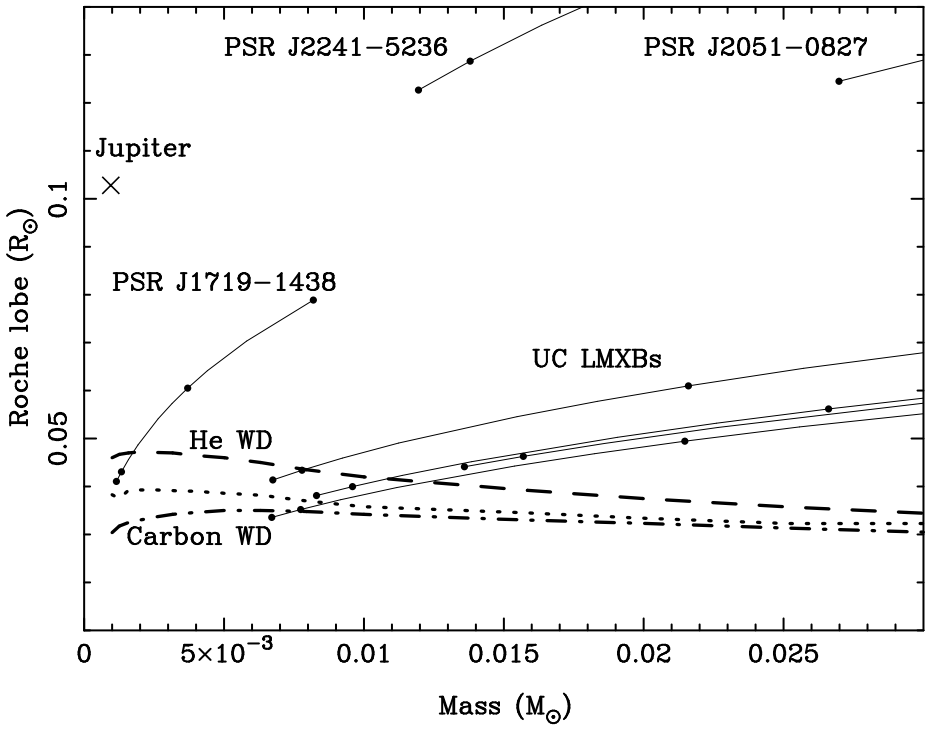

Figure B.2. The locus of the companion mass and Roche Lobe radii for PSR J1719−1438, selected ultra-compact LMXBs and black widow millisecond pulsars for different assumed orbital inclinations. The minimum companion mass and Roche Lobe radii correspond to $i = 90^o$ and a pulsar mass of 1.4 $M_\odot$. As the unknown angle of inclination decreases, the companion mass and radius increase, becoming increasingly improbable. The bullets from lowest to highest mass represent the minimum ($i = 90^o$), median($i = 60^o$), 5% and 1% a priori probabilities that a randomly-oriented inclination would result in the mass and radii at least as high as that indicated. The zero-temperature mass-radius relations from Deloye & Bildsten (2003) are also shown for low-mass He and Carbon white dwarfs. The dotted line represents the mass-radius relation for low-mass Carbon white dwarfs computed by Lai et al. (1991). For reference the mass and radius of Jupiter is shown with an X.

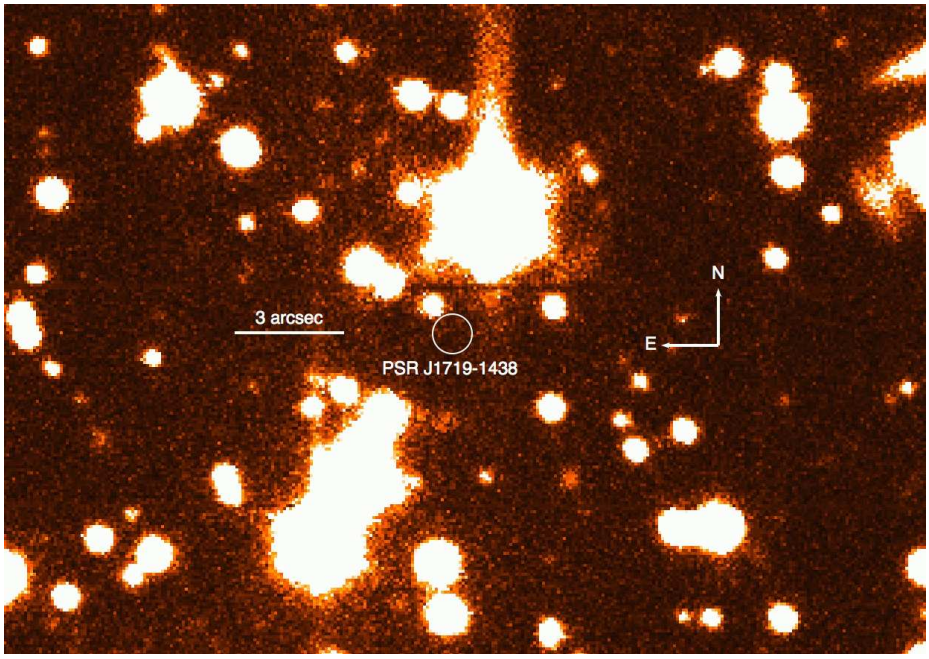

Figure B.3. Keck/LRIS 20 minute R-band image centred on the location of PSR J1719−1438. The image was constructed from 5 exposures taken during the expected maximum luminosity of the companion in a total integration time of 1200s.

Bibliography

Abdo, A. A., Ackermann, M., Ajello, M., Atwood, W. B., Axelsson, M., et al. 2010, The Astrophysical Journal Supplement Series, 187, 460

Agrawal, P. 2006, Advances in Space Research, 38, 2989

Alpar, M. A., Cheng, A. F., Ruderman, M. A., & Shaham, J. 1982, Nature, 300, 728

Arzoumanian, Z., Cordes, J. M., & Wasserman, I. 1999, The Astrophysical Journal, 520, 696

Bailes, M., Bates, S. D., Bhalerao, V., Bhat, N. D. R., Burgay, M., et al. 2011, Science, 1

Barthelmy, S. D., Barbier, L. M., Cummings, J. R., Fenimore, E. E., Gehrels, N., et al. 2005, Space Science Reviews, 120, 143

Barziv, O., Kaper, L., Van Kerkwijk, M. H., Telting, J. H., & Van Paradijs, J. 2001, Astronomy and Astrophysics, 377, 925

Bessell, M. S., Castelli, F., & Plez, B. 1998, Astronomy and Astrophysics, 250, 231

Bhalerao, V. B., & Kulkarni, S. R. 2011, The Astrophysical Journal, 737, L1

Bhalerao, V. B., van Kerkwijk, M. H., Harrison, F. A., Kasliwal, M. M., Kulkarni, S. R., & Rana, V. R. 2010, The Astrophysical Journal, 721, 412

Bhattacharya, D., & van den Heuvel, E. P. J. 1991, Physics Reports, 203, 1

Bildsten, L. 1998, The Astrophysical Journal, 501, L89

—. 2003, Radio Pulsars, 302

Blackburn, J. K. 1995, Astronomical Data Analysis Software and Systems IV, 77

Bolotnikov, A., Cook, W., Harrison, F., Wong, A.-S., Schindler, S., & Eichelberger, A. 1999, Nuclear Instruments and Methods in Physics Research Section A: Accelerators, Spectrometers, Detectors and Associated Equipment, 432, 326

Bonnet-Bidaud, J. M., & Mouchet, M. 1998, Astronomy and Astrophysics, 12, 9

Bonsema, P. F. J., & van den Heuvel, E. P. J. 1985, Astronomy and Astrophysics, 146

Brott, I., de Mink, S. E., Cantiello, M., Langer, N., de Koter, A., et al. 2011, Astronomy & Astrophysics, 530, A115

Camero Arranz, A., Wilson, C. A., Finger, M. H., & Reglero, V. 2007, Astronomy and Astrophysics, 473, 551

Camilo, F., Thorsett, S. E., & Kulkarni, S. R. 1994, The Astrophysical Journal, 421, L15

Casares, J., Hernández, J. I. G., Israelian, G., & Rebolo, R. 2010, Monthly Notices of the Royal Astronomical Society, 401, 2517

Cenko, S. B., Fox, D. B., Moon, D., Harrison, F. A., Kulkarni, S. R., et al. 2006, Publications of the Astronomical Society of the Pacific, 118, 1396

Chabrier, G., Brassard, P., Fontaine, G., & Saumon, D. 2000, The Astrophysical Journal, 543, 216

Chaty, S. 2011, Evolution of compact binaries. Proceedings of a workshop held at Hotel San Martín, 447

Chaty, S., Zurita Heras, J. A., & Bodaghee, A. 2010, eprint arXiv:1012.2318

Christensen, F. E., Hornstrup, A., Westergaard, N. J., Schnopper, H. W., Wood, J., & Parker, K. 1992, In: Multilayer and grazing incidence X-ray/EUV optics; Proceedings of the Meeting, 160

Christensen, F. E., Jakobsen, A. C., Brejnholt, N. F., Madsen, K. K., Hornstrup, A., et al. 2011, in Society of Photo-Optical Instrumentation Engineers (SPIE) Conference Series, Vol. 8147, 81470U–81470U–19

Clark, D. J., Hill, A. B., Bird, A. J., McBride, V. A., Scaringi, S., & Dean, A. J. 2009, Monthly Notices of the Royal Astronomical Society: Letters, 399, L113

Clark, J. S., Goodwin, S. P., Crowther, P. A., Kaper, L., Fairbairn, M., Langer, N., & Brocksopp, C. 2002, Astronomy and Astrophysics, 392, 909

Cordes, J. M., & Lazio, T. J. W. 2002, eprint arXiv:astro-ph/0207156

Cox, A. N. 2000, Allen's astrophysical quantities

Cropper, M. 1990, Space Science Reviews, 54, 195

de Vaucouleurs, G., de Vaucouleurs, A., Corwin, Herold G., J., Buta, R. J., Paturel, G., & Fouque, P. 1991, Volume 1-3, 1

Deloye, C. J., & Bildsten, L. 2003, The Astrophysical Journal, 598, 1217

Demorest, P. B., Pennucci, T., Ransom, S. M., Roberts, M. S. E., & Hessels, J. W. T. 2010, Nature, 467, 1081

Denisenko, D. V., Kryachko, T. V., & Satovskiy, B. L. 2009, The Astronomer's Telegram

Drave, S. P., Bird, A. J., Townsend, L. J., Hill, A. B., McBride, V. A., Sguera, V., Bazzano, A., & Clark, D. J. 2012, Astronomy & Astrophysics, 539, A21

Edwards, R., Bailes, M., van Straten, W., & Britton, M. 2001, Monthly Notices of the Royal Astronomical Society, 326, 358

Eggleton, P. P. 1983, The Astrophysical Journal, 268, 368

Figueira, P., Pepe, F., Lovis, C., & Mayor, M. 2010, Astronomy and Astrophysics, 515, A106

Frank, J., King, A. R., & Raine, D. J. 1985, Accretion power in astrophysics

Freedman, W. L., Madore, B. F., Gibson, B. K., Ferrarese, L., Kelson, D. D., et al. 2001, The Astrophysical Journal, 553, 47

Freire, P. C. C., Ransom, S. M., Bégin, S., Stairs, I. H., Hessels, J. W. T., Frey, L. H., & Camilo, F. 2008, The Astrophysical Journal, 675, 670

Fruchter, A. S., Stinebring, D. R., & Taylor, J. H. 1988, Nature, 333, 237

Galloway, D. K., Chakrabarty, D., Morgan, E. H., & Remillard, R. A. 2002, The Astrophysical Journal, 576, L137

Gehrels, N., Chincarini, G., Giommi, P., Mason, K. O., Nousek, J. A., et al. 2004, The Astrophysical Journal, 611, 1005

Giacconi, R., Gursky, H., Paolini, F., & Rossi, B. 1962, Physical Review Letters, 9, 439

Giacconi, R., Branduardi, G., Briel, U., Epstein, A., Fabricant, D., et al. 1979, The Astrophysical Journal, 230, 540

Gray, D. F. 2005, The Observation and Analysis of Stellar Photospheres

Grindlay, J. E., & Bailyn, C. D. 1988, Nature, 336, 48

Hailey, C. J., An, H., Blaedel, K. L., Brejnholt, N. F., Christensen, F. E., et al. 2010, in Space Telescopes and Instrumentation 2010: Ultraviolet to Gamma Ray. Edited by Arnaud, Vol. 7732, 77320T–77320T–13

Hansen, B. M. S., Shih, H.-Y., & Currie, T. 2009, The Astrophysical Journal, 691, 382

Harrison, F. A., Christensen, F. E., Craig, W., Hailey, C., Baumgartner, W., et al. 2006, Experimental Astronomy, 20, 131

Harrison, F. A., Boggs, S., Christensen, F., Craig, W., Hailey, C., et al. 2010, in Space Telescopes and Instrumentation 2010: Ultraviolet to Gamma Ray. Edited by Arnaud, Vol. 7732, 77320S–77320S–8

Harrison, M., McGregor, D., & Doty, F. 2008, Physical Review B, 77

Harwit, M. 2003, Physics Today, 56, 38

Hellier, C. 2001, Cataclysmic Variable Stars

—. 2002, The Physics of Cataclysmic Variables and Related Objects, 261

Hessels, J., Ransom, S., Roberts, M., Kaspi, V., Livingstone, M., Tam, C., & Crawford, F. 2005, Binary Radio Pulsars, 328

Hessels, J. W. T., Ransom, S. M., Stairs, I. H., Freire, P. C. C., Kaspi, V. M., & Camilo, F. 2006, Science (New York, N.Y.), 311, 1901

Hilditch, R. W. 2001, An Introduction to Close Binary Stars, 1st edn. (Cambridge, UK: Cambridge University Press)

Hilditch, R. W., Howarth, I. D., & Harries, T. J. 2005, Monthly Notices of the Royal Astronomical Society, 357, 304

Hulleman, F., in 't Zand, J. J. M., & Heise, J. 1998, Astronomy and Astrophysics, 337, L25

in 't Zand, J. J. M. 2005, Astronomy and Astrophysics, 441, L1

Iniewski, K. 2010, Semiconductor radiation detection systems (Boca Raton FL: CRC Press/Taylor & Francis)

Jacoby, B. A., Hotan, A., Bailes, M., Ord, S., & Kulkarni, S. R. 2005, The Astrophysical Journal, 629, L113

Jahoda, K., Swank, J. H., Giles, A. B., Stark, M. J., Strohmayer, T., Zhang, W., & Morgan, E. H. 1996, Proc. SPIE Vol. 2808, 2808, 59

Jester, S., Schneider, D. P., Richards, G. T., Green, R. F., Schmidt, M., et al. 2005, The Astronomical Journal, 130, 873

Joss, P. C., & Rappaport, S. A. 1984, Annual Review of Astronomy and Astrophysics, 22, 537

Juett, A. M., Psaltis, D., & Chakrabarty, D. 2001, The Astrophysical Journal, 560, L59

Kaspi, V. M., Lyne, A. G., Manchester, R. N., Crawford, F., Camilo, F., et al. 2000, The Astrophysical Journal, 543, 321

Kaur, R., Wijnands, R., Paul, B., Patruno, A., & Degenaar, N. 2010, Monthly Notices of the Royal Astronomical Society, 402, 2388

Keith, M. J., Jameson, A., Van Straten, W., Bailes, M., Johnston, S., et al. 2010, Monthly Notices of the Royal Astronomical Society, 409, 619

Keith, M. J., Johnston, S., Ray, P. S., Ferrara, E. C., Saz Parkinson, P. M., et al. 2011, Monthly Notices of the Royal Astronomical Society, 414, 1292

Kiziltan, B., Kottas, A., & Thorsett, S. E. 2010, eprint arXiv:1011.4291

Kiziltan, B., & Thorsett, S. E. 2010, The Astrophysical Journal, 715, 335

Knigge, C., Coe, M. J., & Podsiadlowski, P. 2011, Nature, 479, 372

Kolb, U., King, A. R., & Baraffe, I. 2001, Monthly Notices of the Royal Astronomical Society, 321, 544

Kzlolu, U., Kzlolu, N., Baykal, A., Yerli, S. K., & Özbey, M. 2007, Astronomy and Astrophysics, 470, 1023

Lai, D., Abrahams, A. M., & Shapiro, S. L. 1991, The Astrophysical Journal, 377, 612

Landsman, W. B. 1993, Astronomical Data Analysis Software and Systems II, 52

Lang, D., Hogg, D. W., Mierle, K., Blanton, M., & Roweis, S. 2010, The Astronomical Journal, 139, 1782

Lattimer, J., & Prakash, M. 2005, Physical Review Letters, 94

Lattimer, J. M., & Prakash, M. 2004, Science (New York, N.Y.), 304, 536

—. 2007, Physics Reports, 442, 109

Lattimer, J. M., Prakash, M., Day, R. R., & Year, M. 2010, eprint arXiv:1012.3208, 1

Law, N. M., Kulkarni, S. R., Dekany, R. G., Ofek, E. O., Quimby, R. M., et al. 2009, Publications of the Astronomical Society of the Pacific, 121, 1395

Lebrun, F., Leray, J. P., Lavocat, P., Crtolle, J., Arqus, M., et al. 2003, Astronomy and Astrophysics, 411, L141

Lin, J., Rappaport, S., Podsiadlowski, P., Nelson, L., Paxton, B., & Todorov, P. 2011, The Astrophysical Journal, 732, 70

Liu, Q. Z., van Paradijs, J., & van den Heuvel, E. P. J. 2005, Astronomy and Astrophysics, 442, 1135

—. 2006, Astronomy and Astrophysics, 455, 1165

Longair, M. S. 1992, High Energy Astrophysics

Madsen, K. K., Harrison, F. a., Mao, P. H., Christensen, F. E., Jensen, C. P., Brejnholt, N., Koglin, J., & Pivovaroff, M. J. 2009, Proceedings of SPIE, 7437, 743716

Manchester, R. N., Hobbs, G. B., Teoh, A., & Hobbs, M. 2005, The Astronomical Journal, 129, 1993

Mao, P. H., Harrison, F. A., Windt, D. L., & Christensen, F. E. 1999, Applied Optics, 38, 4766

Markwardt, C. B. 2009, Astronomical Data Analysis Software and Systems XVIII ASP Conference Series, 411

Mason, A. B., Clark, J. S., Norton, A. J., Crowther, P. A., Tauris, T. M., Langer, N., Negueruela, I., & Roche, P. 2011a, Monthly Notices of the Royal Astronomical Society, 000, 10

Mason, A. B., Norton, A. J., Clark, J. S., Negueruela, I., & Roche, P. 2011b, Astronomy & Astrophysics, 532, A124

Mason, A. B., Norton, A. J., Clark, J. S., Roche, P., & Negueruela, I. 2010, Société Royale des Sciences de Liège, 80, 699

Massey, P., Morrell, N. I., Neugent, K. F., Penny, L. R., Eastwood, K.-D., & Gies, D. R. 2012, Physics

McCarthy, J. K., Cohen, J. G., Butcher, B., Cromer, J., Croner, E., et al. 1998, Proc. SPIE Vol. 3355, 3355, 81

McConnachie, A. W., Irwin, M. J., Ferguson, A. M. N., Ibata, R. A., Lewis, G. F., & Tanvir, N. 2005, Monthly Notices of the Royal Astronomical Society, 356, 979

McLean, I. S., McGovern, M. R., Burgasser, A. J., Kirkpatrick, J. D., Prato, L., & Kim, S. S. 2003, The Astrophysical Journal, 596, 561

McLean, I. S., Becklin, E. E., Bendiksen, O., Brims, G., Canfield, J., et al. 1998, Proc. SPIE Vol. 3354, 3354, 566

Mighell, K. J. 1999, Astronomical Data Analysis Software and Systems VIII, 172

Munari, U., Sordo, R., Castelli, F., & Zwitter, T. 2005, Astronomy and Astrophysics, 442, 1127

MunozDarias, T., Casares, J., & MartinezPais, I. G. 2005, The Astrophysical Journal, 635, 502

Negueruela, I., & Schurch, M. P. E. 2007, Astronomy and Astrophysics, 461, 631

Niemela, A., & Sipila, H. 1994, IEEE Transactions on Nuclear Science, 41, 1054

Nomoto, K. 1984, The Astrophysical Journal, 277, 791

Oke, J. B., & Gunn, J. E. 1982, Publications of the Astronomical Society of the Pacific, 94, 586

Oke, J. B., Cohen, J. G., Carr, M., Cromer, J., Dingizian, A., et al. 1995, Publications of the Astronomical Society of the Pacific, 107, 375

Özel, F., Psaltis, D., Narayan, R., & McClintock, J. E. 2010, The Astrophysical Journal, 725, 1918

Özel, F., Psaltis, D., Narayan, R., & Villarreal, A. S. 2012, arXiv eprint

Paczynski, B. 1971, Annual Review of Astronomy and Astrophysics, 9, 183

Paul, B., & Naik, S. 2011, Bulletin of the Astronomical Society of India, 39, 429

Pellizza, L. J., Chaty, S., & Negueruela, I. 2006, Astronomy and Astrophysics, 455, 653

Pietsch, W., Misanovic, Z., Haberl, F., Hatzidimitriou, D., Ehle, M., & Trinchieri, G. 2004, Astronomy and Astrophysics, 426, 11

Pietsch, W., Plucinsky, P. P., Haberl, F., Shporer, A., & Mazeh, T. 2006, The Astronomer's Telegram, 905, 1

Pietsch, W., Haberl, F., Gaetz, T. J., Hartman, J. D., Plucinsky, P. P., et al. 2009, The Astrophysical Journal, 694, 449

Podsiadlowski, P. 1993, in Planets around pulsars; Proceedings of the Conference, ed. J. A. Phillips, S. E. Thorsett, & S. R. Kulkarni, Vol. 36, 149–165

Poole, T. S., Breeveld, A. A., Page, M. J., Landsman, W., Holland, S. T., et al. 2007, Monthly Notices of the Royal Astronomical Society, 383, 627

Quaintrell, H., Norton, A. J., Ash, T. D. C., Roche, P., Willems, B., Bedding, T. R., Baldry, I. K., & Fender, R. P. 2003, Astronomy and Astrophysics, 401, 313

Radhakrishnan, V., & Srinivasan, G. 1982, Current Science, 51, 1096

Rahoui, F., Chaty, S., Lagage, P.-O., & Pantin, E. 2008, Astronomy and Astrophysics, 484, 801

Ramsay, G., Cropper, M., Wu, K., Mason, K. O., Córdova, F. A., & Priedhorsky, W. 2004, Monthly Notices of the Royal Astronomical Society, 350, 1373

Rappaport, S., Podsiadlowski, P., Joss, P. C., Di Stefano, R., & Han, Z. 1995, Monthly Notices of the Royal Astronomical Society, 273, 731

Rappaport, S. A., & Joss, P. C. 1983, IN: Accretion-driven stellar X-ray sources (A84-35577 16-90). Cambridge and New York, 1

Rasio, F. A., Shapiro, S. L., & Teukolsky, S. A. 1992, Astronomy and Astrophysics (ISSN 0004-6361), 256

Reig, P. 2011, Astrophysics and Space Science, 332, 1

Reig, P., Negueruela, I., Fabregat, J., Chato, R., Blay, P., & Mavromatakis, F. 2004, Astronomy and Astrophysics, 421, 673

Remillard, R. A., & McClintock, J. E. 2006, Annual Review of Astronomy and Astrophysics, 44, 49

Rephaeli, Y., Nevalainen, J., Ohashi, T., & Bykov, A. M. 2008, Space Science Reviews, 134, 71

Roberts, M. S. E., Gotthelf, E. V., Halpern, J. P., Brogan, C. L., & Ransom, S. M. 2007, Proceedings of the 363. WE-Heraeus Seminar on Neutron Stars and Pulsars 40 years after the discovery. Edited by W. Becker and H. H. Huang. MPE-Report 291. ISSN 0178-0719. Published by the Max Planck Institut für extraterrestrische Physik

Rockosi, C., Stover, R., Kibrick, R., Lockwood, C., Peck, M., et al. 2010, in Ground-based and Airborne Instrumentation for Astronomy III. Edited by McLean, Vol. 7735, 77350R–77350R–11

Schlegel, D. J., Finkbeiner, D. P., & Davis, M. 1998, The Astrophysical Journal, 500, 525

Schwab, J., Podsiadlowski, P., & Rappaport, S. 2010, The Astrophysical Journal, 719, 722

Shevchuk, A. S., Fox, D. B., Turner, M., & Rutledge, R. E. 2009, The Astronomer's Telegram

Shklovskii, I. S. 1970, Soviet Astronomy, 13

Shporer, A., Hartman, J., Mazeh, T., & Pietsch, W. 2006, The Astronomer's Telegram, 913, 1

Sidoli, L. 2011, Advances in Space Research, 48, 88

Simcoe, R. A., Metzger, M. R., Small, T. A., & Araya, G. 2000, American Astronomical Society, 32

Smith, D. M. 2004, The Astronomer's Telegram

Stappers, B. W., Bailes, M., Manchester, R. N., Sandhu, J. S., & Toscano, M. 1998, The Astrophysical Journal, 499, L183

Stappers, B. W., van Kerkwijk, M. H., Lane, B., & Kulkarni, S. R. 1999, The Astrophysical Journal, 510, L45

Steidel, C. C., Shapley, A. E., Pettini, M., Adelberger, K. L., Erb, D. K., Reddy, N. A., & Hunt, M. P. 2004, The Astrophysical Journal, 604, 534

Steiner, A. W., Lattimer, J. M., & Brown, E. F. 2010, The Astrophysical Journal, 722, 33

Sunyaev, R. A., Grebenev, S. A., Lutovinov, A. A., Rodriguez, J., Mereghetti, S., Gotz, D., & Courvoisier, T. 2003, The Astronomer's Telegram, 190, 1

Takahashi, T., Abe, K., Endo, M., Endo, Y., Ezoe, Y., et al. 2007, Publications of the Astronomical Society of Japan

Tauris, T. M., Langer, N., & Kramer, M. 2011, Monthly Notices of the Royal Astronomical Society, 416, 2130

Timmes, F. X., Woosley, S. E., & Weaver, T. A. 1996, The Astrophysical Journal, 457, 834

Torres, G. 2010, The Astronomical Journal, 140, 1158

Toscano, M., Sandhu, J. S., Bailes, M., Manchester, R. N., Britton, M. C., Kulkarni, S. R., Anderson, S. B., & Stappers, B. W. 1999, Monthly Notices of the Royal Astronomical Society, 307, 925

Tousey, R., Watanabe, K., & Purcell, J. 1951, Physical Review, 83, 792

Ubertini, P., Lebrun, F., Di Cocco, G., Bazzano, A., Bird, A. J., et al. 2003, Astronomy and Astrophysics, 411, L131

Valentim, R., Rangel, E., & Horvath, J. E. 2011, Monthly Notices of the Royal Astronomical Society, 414, 1427

van den Heuvel, E. P. J., & Bonsdema, P. T. J. 1984, Astronomy and Astrophysics (ISSN 0004-6361), 139

van der Meer, A., Kaper, L., van Kerkwijk, M. H., Heemskerk, M. H. M., & van den Heuvel, E. P. J. 2007, Astronomy and Astrophysics, 473, 523

van Dokkum, P. G. 2001, Publications of the Astronomical Society of the Pacific, 113, 1420

van Kerkwijk, M. H., Breton, R. P., & Kulkarni, S. R. 2011, The Astrophysical Journal, 728, 95

van Kerkwijk, M. H., van Paradijs, J., Zuiderwijk, E. J., Hammerschlag-Hensberge, G., Kaper, L., & Sterken, C. 1995, Astronomy and Astrophysics

Verbiest, J. P. W., Bailes, M., van Straten, W., Hobbs, G. B., Edwards, R. T., et al. 2008, The Astrophysical Journal, 679, 675

Voges, W., Aschenbach, B., Boller, T., Bräuninger, H., Briel, U., et al. 1999, Astronomy and Astrophysics

Walborn, N. R., & Fitzpatrick, E. L. 1990, Publications of the Astronomical Society of the Pacific, 102, 379

Warner, B. 1995, Camb. Astrophys. Ser., 28

Weisskopf, M. C., Tananbaum, H. D., Van Speybroeck, L. P., & O'Dell, S. L. 2000, Proc. SPIE Vol. 4012, 4012, 2

Wijers, R. A. M. J., van den Heuvel, E. P. J., van Kerkwijk, M. H., & Bhattacharya, D. 1992, Nature, 355, 593

Wilson, C. A., Finger, M. H., Harmon, B. A., Chakrabarty, D., & Strohmayer, T. 1998, The Astrophysical Journal, 499, 820

Wilson, C. A., Weisskopf, M. C., Finger, M. H., Coe, M. J., Greiner, J., Reig, P., & Papamastorakis, G. 2005, The Astrophysical Journal, 622, 1024

Wolszczan, A., & Frail, D. A. 1992, Nature, 355, 145

Wolter, H. 1952a, Annalen der Physik, 445, 286

—. 1952b, Annalen der Physik, 445, 94

York, D. G., Adelman, J., Anderson, J., Anderson, S. F., Annis, J., et al. 2000, The Astronomical Journal, 120, 1579

Zhang, C. M., Wang, J., Zhao, Y. H., Yin, H. X., Song, L. M., et al. 2011, Astronomy & Astrophysics, 527, A83

Zwitter, T., Castelli, F., & Munari, U. 2004, Astronomy and Astrophysics, 417, 1055